SRL Record Copy

√ 27 4665

DP-1606
Revision 2

DEFENSE WASTE PROCESSING FACILITY WASTEFORM AND CANISTER DESCRIPTION

Richard G. Baxter

E. I. du Pont de Nemours & Co.
Savannah River Plant
Aiken, SC 29808

PREPARED FOR THE U.S. DEPARTMENT OF ENERGY UNDER CONTRACT DE-AC09-76SR00001

Printed in the United States of America

Available from

National Technical Information Service
U. S. Department of Commerce
5285 Port Royal Road
Springfield, Virginia 22161

Price: Printed Copy A04; Microfiche A01

DP-1606
Rev 2
Distribution Category UC-721

DEFENSE WASTE PROCESSING FACILITY WASTEFORM AND CANISTER DESCRIPTION

RICHARD G. BAXTER

Approved by

Lucien M. Papouchado, Program Manager,
Waste Management Programs

Publication Date: December 1988

E. I. du Pont de Nemours & Co.
Savannah River Plant
Aiken, SC 29808

PREPARED FOR THE U. S. DEPARTMENT OF ENERGY UNDER CONTRACT DE-AC-09-76SR00001

Acknowledgments

Many persons in the Savannah River Laboratory and Plant are responsible for the data in this report. In particular, the contributions of John R. Fowler and Richard E. Edwards for material and curie balances, and M. John Plodinec for glass chemistry and leachability, were important to the preparation of this document.

ABSTRACT

This document describes the reference wasteform and canister for the Defense Waste Processing Facility (DWPF) and updates DP-1606, Rev. 1, which was published in August 1983. The principal changes include revised feed and glass product compositions, an estimate of glass product characteristics as a function of time after the start of vitrification, and additional data on glass leaching performance. The feed and glass product composition data are identical to that described in the DWPF Basic Data Report, Revision 90/91 (see references).

The DWPF facility is located at the Savannah River Plant in Aiken, SC, and it is scheduled for construction completion during December 1989.

The wasteform is borosilicate glass containing approximately 28 wt % sludge oxides, with the balance consisting of glass-forming chemicals, primarily glass frit. Borosilicate glass was chosen because of its stability toward reaction with potential repository groundwaters, its relatively high ability to incorporate nuclides found in the sludge into the solid matrix, and its reasonably low melting temperature. The glass frit contains approximately 71% SiO_2, 12% B_2O_3, and 10% Na_2O.

Tests to quantify the stability of DWPF waste glass have been performed under a wide variety of conditions, including simulations of potential repository environments. Based on these tests, DWPF waste glass should easily meet repository criteria.

The canister is filled with about 3,700 lb of glass which occupies 85% of the free canister volume. The filled canister will generate approximately 690 watts when filled with oxides from 5-year-old sludge and precipitate from 15-year-old supernate. The radionuclide activity of the canister is about 233,000 curies, with an estimated radiation level of 5,600 rad/hour at the canister surface.

The canister is fabricated of standard 24 in. OD, schedule 20, type 304L stainless steel pipe with a dished bottom, domed head, and a combined lifting and welding flange on the head nozzle. The overall canister length is 9 ft. 10 in. (300 cm) with a wall thickness of 3/8 in. The canister length was selected to establish a practical cell height in the DWPF. The canister diameter was selected as an optimum size from glass quality considerations, a logical size for repository handling, and to ensure that a filled canister in either a single- or a double-containment shipping cask could be accommodated on a legal-weight truck. The overall dimensions and weight are compatible with repository requirements.

CONTENTS

Introduction 9

High Level Wasteform Characteristics 9

Composition of DWPF Waste Glass 9

Physical Properties of DWPF Waste Glass 11

Chemical Stability of DWPF Waste Glass 12

DWPF Canister 15

Estimated Production Schedule 20

References 21

Figures 26

Tables 36

LIST OF FIGURES

1 Calculated True Specific Heat of DWPF Glass 26

2 Calculated Density of DWPF Glass 26

3 Calculated Thermal Conductivity of DWPF Glass 27

4 Experimental Resistivity of DWPF Glass 27

5 Experimental Thermal Expansion Data for Simulated Waste Glass, Simulation 1 28

6 Experimental Thermal Expansion Data for Simulated Waste Glass, Simulation 2 28

7 Experimental Thermal Expansion Data for Simulated Waste Glass, Simulation 3 29

8 Experimental Viscosity of DWPF Glass 29

9 Durability of Glasses and Minerals in an MCC-1 Leach Test 30

10 Repository Simulation Test Vessels 30

11 Results from 2-Year Burial Experiments 31

12 Effect of Melter Size on Glass Leaching 31

13 Canister Grapple 32

14 Canister Assembly 33

15 Sludge-Precipitate Canister Decay Heat 34

16 Sludge-Precipitate Canister Activity 35

LIST OF TABLES

1A Chemical Composition of Sludge Feed Soluble Solids 36

1B Chemical Composition of Sludge Feed Insoluble Solids 37

2 Radionuclide Content of Sludge Feed 38

3 Partial Isotopic Content of Sludge Feed 39

4 Chemical Composition of Precipitate Feed from In-Tank Processing to Salt Cell 41

5 Radionuclide Content of Precipitate Slurry Feed to the Salt Cell 42

6 Partial Isotopic Content of Precipitate Slurry Feed to the Salt Cell 43

7 Chemical Composition of Feed from Salt Cell 45

8 Radionuclide Content of Feed from Salt Cell 46

9 Partial Isotopic Content of Feed from Salt Cell 47

10 Chemical Composition of Sludge-Precipitate Glass 49

11 Radionuclide Content of Sludge-Precipitate Glass 50

12 Partial Isotopic Content of Sludge-Precipitate Glass 51

13A Chemical Composition of Glass Frits 53

13B Projected DWPF Waste Glass Compositions 54

14 Physical Properties of Glass Wasteforms 55

15 Composition of Simulated Wastes 55

16 Heat Capacities of Simulated Waste Glasses 56

17 Measured Density of SRP Simulated Waste Glasses 57

18 Zeolite Composition 57

19 Canister Decay Heat and Activity 58

20 Radiation from Canister of Sludge-Precipitate Glass 59

21 Chemical Composition of Sludge-Precipitate Glass for Radiation Calculations 59

22 Source Terms for Sludge-Precipitate Glass for Radiation Calculations 60

LIST OF TABLES, (contd)

23 Major Contributing Isotopes to Gamma Dose Rates 61

24 Gamma Radiation from Canister - Comparison of Calculations 61

25 Neutron Radiation from Canister - Comparison of Calculations 62

26 Reference Canister Temperatures 62

27 Projected Waste Inventory and Fission Product Radioactivity as of December 31, 1988 63

28 Estimated Production Schedule and Estimated Cumulative Average Radioactivity and Thermal Power per Canister of HLW Glass 64

DEFENSE WASTE PROCESSING FACILITY
WASTEFORM AND CANISTER DESCRIPTION

INTRODUCTION

This document describes the reference glass wasteform and canister for the Defense Waste Processing Facility (DWPF). The borosilicate glass wasteform and stainless steel canister are the reference package selected in December 1982, and they are the basis for the DWPF design and process.

HIGH LEVEL WASTEFORM CHARACTERISTICS

The wasteform for the DWPF is a borosilicate glass containing approximately 28% sludge oxides with the balance consisting of glass-forming chemicals, primarily glass frit. Borosilicate glass was chosen as a wasteform because of its stability toward attack by water, its relatively high ability to dissolve nuclides found in the sludge into the melt, its relatively low melting temperature, and because the process is based on well-developed technology.

Description of the waste glass characteristics is divided into three sections: composition, mechanical properties, and chemical stability. Sludge-precipitate processing is based on processing the 5-year-old or older sludge plus a 15-year-old or older supernate fraction. The sludge fraction contains the strontium and plutonium, and the supernate portion contains virtually all of the cesium. Mechanical properties of the waste glass are based on a typical frit, designated as Frit 131.* Other frits, such as Frits 165 and 200, have similar mechanical properties, based on experimental laboratory tests.

Data on the stability of waste glasses described in this report are from glasses simulating the DWPF product, which are based on Frit 165. Although the glasses produced in the DWPF will not be identical to glasses made from Frit 165, due to changes in the DWPF process after the development of Frit 165, the chemical stability is expected to be similar, based on experimental laboratory tests (see Glass Stability Programs under References).

COMPOSITION OF DWPF WASTE GLASS

Feed to the DWPF consists of two streams: settled, washed sludge and supernatant liquid. The sludge consists of hydroxides and hydrous oxides containing nearly all of the stable and radioactive fission products, and actinide elements, as well as elements added in the SRP separations processes. These are primarily iron, manganese, aluminum, and mercury. The sludge is treated with sodium hydroxide to dissolve hydrated aluminum oxides, washed with water to remove soluble salts to 2% on a dry basis, and then allowed to settle. The washed sludge is transferred as a 13% slurry to the DWPF slurry receipt adjustment tank (SRAT).

*Savannah River Laboratory frit designations.

The supernate solution containing dissolved salts is treated in the waste tanks with sodium tetraphenylborate to precipitate cesium, and with sodium titanate to absorb the trace amounts of strontium and plutonium compounds present in the supernate. These precipitates are transferred to the DWPF salt processing cell where the organic portion of the salts are decomposed to benzene and the inorganic portion is transferred to the slurry receipt adjustment tank.

Sludge Processing

A description of the chemical composition of sludge feed is shown in Tables 1A and 1B, the radionuclide content in Table 2, and the isotopic content in Table 3. The soluble solids (Table 1A) are principally $NaNO_3$ (41%), $NaNO_2$ (19%), NaOH (18%), and $NaAl(OH)_4$ (11%), which constitute about 89% of the soluble solids. Of the insolubles (Table 1B; zeolite composition is given in Table 18), $Fe(OH)_3$ (41%), $Al(OH)_3$ (16%), MnO_2 (7%), and $UO_2(OH)_2$ (7%) constitute approximately 70% of the insoluble solids. Activity of the sludge feed is 133 Ci/gal (Table 2) with a decay heat of 0.44 watt/gal for 5-year-old waste. Of this activity, 78% is due to Sr-90, Y-90, and Pm-147.

Precipitate Processing

A description of the chemical composition of the precipitate feed to the salt cell is shown in Table 4, the radionuclide content of feed from the precipitate process is shown in Table 5, and the isotopic content in Table 6. The principal compounds of the precipitate feed, on a water-free basis, are potassium tetraphenylborate (KTPB) (76%), $NaNO_3$ (6%), and NH_4TBP (4%); these compounds constitute about 85% of the input stream. Activity of the feed from the precipitate process is 71.4 Ci/gal with a decay heat of 0.167 watt/gal for precipitate from 15-year-old supernate. Of this activity, about 99% is due to Cs-137 and its beta decay daughter Ba-137m.

The chemical composition of the feed from the salt cell to the SRAT is shown in Table 7, the radionuclide content in Table 8, and the isotopic content in Table 9. The principal components, on a water-free basis, are KCOOH (29%), H_3BO_3 (19%), and NaCOOH (13%). Activity of this feed to the SRAT is 76.5 Ci/gal with a decay heat of 0.178 watt/gal.

The chemical composition of combined sludge and precipitate waste glass is shown in Table 10, the radionuclide content is shown in Table 11, and the isotopic content in Table 12. Total activity is 63.1 Ci/lb with a decay heat of 0.187 watt/lb for 5-year-old sludge and precipitate from 15-year-old supernate. Thus, the 3,700 lb of glass in a DWPF canister contains about 233,000 Ci with a decay heat of 690 watts. The isotopes Y-90, Sr-90, Cs-137, Ba-137m, and Pm-147 contribute about 87% of the activity.

Chemical composition of the design basis frit, designated as Frit 200, is shown in Table 13A. Composition of the frit to be used during initial operations, Frit 202, is also shown. Frit 202 is approximately 77% SiO_2, 8% B_2O_3, and 7% Li_2O. The frit was developed after an extensive series of tests designed to produce a waste glass product with good leach resistance, high solubility for waste oxides, and a practical melting temperature. It is based on earlier efforts which resulted in the development of Frit 165. The performance of the DWPF glass is expected to be similar to that of Frit 165 glasses, based on experimental laboratory tests. Compositions of glasses expected to be produced by the DWPF are shown in Table 13B.

PHYSICAL PROPERTIES OF DWPF WASTE GLASS

Physical properties of DWPF waste glass have been measured and estimated by calculation. Most of the properties determined by experiment are based upon Frit 165 rather than the Frit 200; however, there are few significant differences. The principal differences between the two are that Frit 200 is higher in percent of SiO_2 and B_2O_3, but contains no ZrO_2. A chemical comparison between several of the frits evaluated is shown in Table 13A.

Physical properties of glass wasteforms are listed in Table 14. Of these values, the fractional thermal expansion, the density at 100°C, and the softening point were experimentally determined for Frit 165 glass. Other values are based on Frit 21 or other typical compositions.

Several other physical properties of SRP waste glasses have been estimated by calculation. Heat capacity, thermal conductivity, and density for three types of DWPF waste glass (composite, high iron, and high aluminum) have been calculated on the basis of glass containing approximately 28% sludge oxides and the balance glass Frit 131. Physical properties of waste glasses made in the range of frit compositions expected in the DWPF showed that these properties were invariant with changes in frit composition. Typical compositions of waste for these three types of glass are shown in Table 15.

Heat Capacity

Measured and calculated heat capacities of simulated waste glasses are listed in Table 16. C_{pt} is the true heat capacity at the indicated temperature. True specific heat as a function of temperature is also shown in Figure 1.

Density

Measured densities for simulated waste glass are listed in Table 17, and density as a function of temperature is shown in Figure 2 for the range of glasses expected in DWPF.

Thermal Conductivity

Calculated thermal conductivity of DWPF glass as a function of temperature is shown in Figure 3.

Electrical Resistivity

Measured electrical resistivity of the glass melt as a function of temperature is shown in Figure 4. At the operating melt temperature of 1,150°C, the resistivity is approximately 2.5 ohm-cm for composite glass.

Thermal Expansion

Waste glass measured thermal expansion as a function of temperature is shown in Figure 5 for composite glass, in Figure 6 for high-Al glass, and in Figure 7 for high-Fe glass.

Viscosity

Experimentally determined viscosities for the range of glasses expected in the DWPF are shown in Figure 8. At the nominal operating temperature of 1,150°C, the composite glass viscosity is about 30 poise.

CHEMICAL STABILITY OF DWPF WASTE GLASS

In accordance with the Nuclear Waste Policy Act of 1982, the canisters of waste glass produced in the DWPF will eventually go to a licensed federal repository for permanent disposal. Recent legislation indicates that the first repository will be in tuff at the Nevada Test Site. At the repository, the canister containing waste glass will be emplaced in the geology as part of a waste package. This package will contain the waste glass, the type 304L stainless steel canister, a metallic overpack to meet the containment requirement of 10 CFR 60, and possibly a packing material such as crushed rock or clay.

Reaction of waste glass with repository groundwater is the most likely mode of release of long-lived radioactive species to the environment. Borosilicate glass was chosen as the wasteform for the DWPF because of its stability when exposed to groundwater. Thus, Savannah River Laboratory (SRL) has focused on developing a quantitative understanding of the reaction between glass and groundwater over the range of conditions expected for liquid groundwater and DWPF glass interactions in candidate repository environments.

The expected range of conditions for each of three geologies is shown in the following table. The ranges have been derived from reference repository conditions for each of the geologies. The values are based on the assumption that the waste package containing DWPF glass in the repository will meet regulatory requirements, particularly the containment requirement imposed by the Nuclear Regulatory Commission in 10 CFR 60.

EXPECTED CONDITIONS FOR INTERACTIONS BETWEEN GROUNDWATER AND DWPF GLASS

PARAMETER	REPOSITORY CONDITION		
	SALT	BASALT	TUFF
Temperature	34 - 90°C	57 - 150°C	30 - 95°C
Pressure	2800 PSI	4700 PSI	Atmosperic
Groundwater	Brine	Silicate	Dilute Silicate
Eh	≈ 0 v	- 0.40 v	Oxidizing
pH	6	9.75	7.5
Flow	Static	Very Slow	Intermittent
Amount	Limited	Flooded	Limited

Studies on glass stability have been in progress at the Savannah River Laboratory for the past ten years. Early glass leaching characteristics of SRP simulated and actual waste glasses are summarized in report DP-1629 (see reference section). These early studies showed that DWPF glass reacted very slowly with groundwaters, and could immobilize the radionuclides in SRP waste. In this section, more recent results are summarized.

The program being carried out by SRL has two major components: mechanistic studies, and verification. SRL's mechanistic studies are directed toward developing a quantifiable model of long-term release from DWPF waste glass, while verification studies test the validity of the model and its predictions. Although these are separate functions, there is necessarily a large amount of interaction between the two components. For example, leaching models are used in the design of verification experiments to point out the appropriate parameters to measure. Conversely, verification

tests can indicate phenomena not considered in the modeling program, and thus are used to guide modeling efforts.

Glass - Groundwater Reaction Mechanisms

The SRL programs to identify and quantify the mechanisms of the reactions between waste glass and repository groundwaters include:

- Fundamental studies designed to quantify the effects of parameters such as glass composition, groundwater composition (including Eh, pH, and dissolved gases), or radiation on glass durability.

- Laboratory tests designed to quantify glass performance under conditions simulating actual potential repository environments.

The first item includes both theoretical and experimental efforts. The thermodynamic approach, first suggested by Paul and Newton, has been an important tool which has enabled SRL to compare the performance of a wide range of glasses and minerals based on their compositions. As Figure 9 shows, the performance of basalt from the Hanford reservation is virtually indistinguishable from that of the DWPF product.

SRL is also performing repository simulation tests in the laboratory, using both actual and simulated waste glasses. These tests are providing data which will be used to determine the stability of DWPF glass in a given repository. In these tests, waste glass and stainless steel samples (simulating a breached canister) are placed in a reaction vessel made from rock representative of one of the candidates for a repository - tuff, basalt, or salt (Figure 10). The reaction vessels used in these experiments are rock cups made from either tuff from outcrops at the Nevada Test Site, basalt from outcrops on the Hanford site, or salt from the WIPP site in New Mexico. Groundwater is then placed in these rock cups, and the cups are closed. For the tests in tuff, actual groundwater from a well (J-13) at the Nevada Test Site is used. In the case of basalt, a synthetic groundwater (GR-4), prepared in an oxygen-free environment, is used. For the salt tests, both inclusion and intrusion brines are used.

Although these laboratory tests are not all completed, they all indicate that the amount of radioactivity which will be free to travel with the groundwater will be a small fraction of the activity present in the waste glass. The results that follow are from the radioactive tests in tuff cups, in terms of concentrations.

In these tuff tests, solution concentrations of most elements were constant within experimental error after approximately 40 days, indicating that the rate of alteration of the glass had become very small. The final concentrations of species in solution were then used to provide estimates for the amount of material released by the waste glass. The concentrations were multiplied by an extremely conservative upper bound for the amount of groundwater which would be available for reaction (50 L), and then divided by the inventory of the individual species. This yielded the estimates of fractional release from these waste packages. The small fractions released are 500 - 1000 times less than the NRC requirement for the waste package as a whole. Similar numbers result from application of mass transfer methodology to the results of these tests. Thus, the tests indicate that DWPF glass should perform well in this environment.

RESULTS OF TUFF SIMULATED REPOSITORY TESTS

SPECIES	FINAL CONCENTRATION	ANNUAL FRACTIONAL RELEASE
Cs	0.9 μg/mL	6×10^{-8}
Sr	2.0	3×10^{-8}
Pu	0.03	1×10^{-8}

Verification Testing

The results and conclusions from SRL's mechanistic efforts are being verified in several ways:

- Extensive testing of waste glass in burial experiments in underground laboratories, to relate performance in the laboratory to the actual repository.
- Large-scale leaching experiments using thick slices from full-scale canisters of simulated waste glass, to relate the performance of laboratory-size samples to that of full-scale canisters of waste glass.
- Extensive testing of simulated and actual waste glasses prepared according to the DWPF process, to relate the performance of laboratory-prepared samples to that of glass made in the DWPF.

The most advanced of these verification programs is that in which samples of simulated waste glass have been buried in underground facilities. Extensive testing has been carried out in the Stripa mine in Sweden, where samples of several simulated waste glasses have been buried in granite for over a year. In this joint effort, scientists from SRL, KBS (the Swedish nuclear program), and the University of Florida have found only a slight interaction between glass and groundwater in the first month of testing, and virtually none thereafter. This agrees well with laboratory tests which also show that steady-state is reached rather quickly. The thermodynamic approach previously alluded to was also applied to these tests, with the results shown in Figure 11. The amount of material released in two years was approximately 50 times less than regulatory limits.

A more extensive set of burial tests has begun in the Waste Isolation Pilot Plant (WIPP) facility in New Mexico. In these tests, samples of simulated waste glasses from seven countries have been emplaced in salt approximately 2,000 feet underground. These samples are being subjected to brine attack under both expected and unexpected but possible conditions in a salt repository.

The relevance of the mechanistic studies have also been verified in other ways. For example, full-scale canisters of nonradioactive simulated waste glass, filled according to the DWPF process in the SRL Engineering Test Facility, have been sliced into sections 18 to 24 inches high. These

large slices were then immersed in large leach vessels of deionized water, and leached under conditions approximating the standard MCC-1 test. A companion set of experiments was performed with laboratory-size samples of the same glass to determine the appropriate relationship between laboratory and full-scale tests. When differences in surface preparation of the samples were removed from the data, there was excellent agreement between the two data sets.

SRL is also continuing to rigorously characterize and test glass samples made according to the DWPF process. The purpose of this effort is to establish that the results of tests of laboratory-prepared samples are relevant to the performance of DWPF glass. For example, samples of glass of the same composition were prepared in a 50 cc crucible, a 3 kg continuous electric melter, and in a 1,500 kg capacity continuous melter, with residence times ranging from 3 to 70 hours. As shown in Figure 12, the performance of the glass did not vary appreciably with the size of the melter. Thus, the performance of DWPF glass actually produced in the DWPF will be similar to that of glass made in the laboratory. Similar studies will determine the effects of other processing variables, such as melt temperature, on the performance of the DWPF product. Ultimately, a response surface model relating process variables to product performance will be generated.

DWPF CANISTER

Canister Grapple Assembly

The lifting grapple is specific for the DWPF canister and was developed by Remote Technology Corp. (REMOTEC) of Oak Ridge, TN (see references). The design is described in detail in the literature, therefore only the principles will be described here. Figure 13 is an assembly drawing..

Maximum size	Diameter =	600 mm
	Length =	1,000 mm
Capacity	6,820 kg, rated.	
Operation	Two-step release, failsafe. Transported by in-cell crane.	
Mechanism	All mechanical.	
Design life	60,000 cycles over 5 years without lubrication.	
Repair	Contact maintenance after high pressure wet decontamination.	
Failure recovery	Manual release activated by 4 kg maximum pull force.	
Materials	Stainless steel.	
Testing	Load test:	125% of rated load
	Cycle test:	500 cycles at rated load
	Misalignment:	Engage canister neck with 25 mm offset from grapple centerline
	Collision:	Strike object with crane traveling at 9 m/min.

Canister Dimensions

Canister dimensions and weight are shown in Figure 14 from drawing W832094 - Rev. 5, "DWPF Canister Assembly".

Principal dimensions and tolerances are:

Overall length	118.00 in. ± 0.06 in.
Outside diameter	24.00 in. ± 0.12 in.
Wall thickness	3/8 in. nominal pipe tolerance
Bow	0.12 in. max
Surface finish	125 rms
Inside volume	26.0 ft^3 nominal
Weight, empty	1100 lb
Weight, 85% full	4800 lb
Material	Type 304L stainless steel

Material of Construction

Type 304L stainless steel was chosen as the canister material for vitrified waste using the continuous melter process. This recommendation is based on long-term heating tests for up to 20,000 hours (2.3 yr) at temperatures that bracket those expected during interim storage. In these tests, the lifetime of canisters containing vitrified waste glass stored in air was predicted. The measured thickness of the reaction layer between the canister alloy and the canister alloy-environment, similar to that expected during interim storage, was extrapolated to estimate the time required for penetration of the 3/8-in thick canister.

Data from tests indicate that a 3/8-in. thick canister of type 304L stainless steel would not be penetrated for more than 8,000 years in a surface facility. By contrast, a 3/8-in. thick low carbon steel canister would be penetrated by oxidation in about 200 years of storage in a surface facility, and its strength would be reduced in a much shorter period.

Differences in canister lifetimes, predicted from these tests, are attributable to the differences in corrosion resistance of the candidate alloys. Both type 304L stainless steel and low carbon steel react similarly with vitrified waste, but type 304L stainless steel is much more resistant to both high temperature and atmospheric corrosion in a radiation field than is low carbon steel. The lifetime of canisters constructed from other compositions of austenitic stainless steels would be expected to be similar to that of type 304L.

Stainless steel has the additional advantage of forming a relatively thin oxide layer when heated by the molten glass. Tests made at Pacific Northwest Laboratory (PNL) indicate that an inert gas blanket would have to be used with a carbon steel canister to reduce the oxide scale formation to less than 22 lb per canister. Furthermore, the stainless steel surface is much easier to decontaminate by blasting with a frit-water slurry than is carbon steel.

The 3/8 in. nominal wall thickness of a 24-in. OD, schedule 20, stainless steel pipe is adequate for DWPF processing. A theoretical stress analysis was made on the reference canister just after it was filled with glass at the instantaneous pour rate of 3.8 lb/min. A maximum wall temperature of 427°C and a maximum bottom temperature of 649°C were assumed. The calculations show that the wall is sufficiently thick to permit the canister to be picked up immediately after it is filled, despite the residual shell hoop stress of 32,500 psi caused by the lower coefficient of thermal expansion of glass compared to that of stainless steel. Furthermore, the hoop stress quickly drops to about

5000 psi (at 500°C) due to the glass moving up into the canister void space as it gradually cools. Similarly, the thermal axial stresses were calculated to be 18,900 psi, and the simple static stresses due to weight were 477 psi shear and 177 psi axial. None of these stress levels indicates the need for a wall thickness greater than 3/8 in.

Canister Weight

The reference design canister is filled with approximately 165 gal of glass (22.1 ft^3) to a fill height of 91 in. This volume corresponds to a nominal weight of 3,700 lb for the current frit (Frit 200) and waste loading, and is about 85% of the available canister volume. The fill volume was chosen based upon operating experience where a 15% void is made available in the event of: low density foam partially filling the canister; "roping" of the glass stream causing voids in the frozen melt; and the possibility of spilling glass on the process room floor due to malfunction of load cells, level instrumentation, failure of pouring equipment, or operator error. After operating experience is gained, it may be possible to fill the canister to the top of the straight section of pipe at the intersection of the head with the cylinder. This volume is 25.3 ft^3 corresponding to a glass weight of 4,200 lb and a fill height of 104 in.

At the completion of pour, the centerline temperature at a point 37 in. from the canister base is about 750°C. At this temperature, the glass density can vary between 2.45 - 3.02 g/cm^3 corresponding to a glass fill weight ranging between 3,380 - 4,170 lb. The glass density variation is a function of the frit composition, waste loading, and waste composition.

Internal Pressurization Potential

Internal pressure within the canister is due to the accumulation of helium from alpha emissions of transuranic nuclides. A DWPF canister filled with waste glass produces about 0.32 cm^3 of helium per year at 40°C. The helium produced is assumed to diffuse through the glass into the void space above the solid glass surface. At the end of 1,000 years, the 103-liter void space pressure has increased by only 0.05 psi. This negligible pressure buildup is of no concern in waste package design. For the case of a canister filled to 25.3 ft^3 (733 L), the 23-liter void space pressure would increase by 0.2 psi.

Seal Weld

The reference process for sealing the canister is to resistance weld a 5-in. dia, 1/2-in. thick, type 304L stainless steel plug into the canister neck. A force of 75,000 lb, a current of 225,000 amps, and a voltage of approximately 10 volts is used to make the 1.5-sec weld. The technique was chosen after consideration of seven alternative processes including gas tungsten arc, gas metal arc, plasma arc, Thermit, electron beam, laser beam, and friction welding, because of the high weld quality and relatively simple equipment required. Weld tensile strength measurements were made on the upset resistance weld under varying conditions of oxidation to determine the need for machining the throat surface after the canister is filled with glass. An upset resistance weld with a 5–in. dia plug and a machine canister neck was leaktight to approximately 10^{-8} atm/cc/sec for a hydrostatic test pressure of 5,000 psi. If the canister neck is heated to 600°C, but not machined before it is welded, then the weld strength as measured by tensile and hydrostatic tests was reduced by about 20%. However, temperature measurements made on the canister neck during glass filling indicate that the maximum neck temperature does not exceed 300°C, so the canister seal weld is capable of withstanding at least 4,000 psi internal pressure while maintaining a leak tightness of 1×10^{-8} atm/cc/sec.

In the event that the canister is used in a repository with a flexible overpack and an open-ended sleeve, the canister could be subjected to relatively high lithostatic or hydrostatic pressures. The maximum pressure in a repository is expected to be less than 18 MPa (2,610 psi) which will buckle the 3/8-in. canister head above the glass melt surface. To prevent buckling, the head could have supporting ribs welded to the head interior or a thicker spherical head could be used. Present repository designs use rigid overpacks which are capable of withstanding repository pressures without collapsing.

Canister Decay Heat and Activity

Table 19 and Figure 15 describe the canister decay heat as a function of time for sludge-precipitate glass over a period of 5 to 1,000 years. The starting point is a sludge age of 5 years combined with precipitate from 15-year-old supernate. Figure 16 shows the canister activity for the same period. After a period of 300 years, the decay heat has decreased to about 7 watts and the activity to about 400 curies.

Fissionable Material Content

The fissionable material content of a sludge-precipitate glass canister is nominally 297 grams for sludge cooled 5 years, and for supernate cooled 15 years. Distribution of the thermal neutron fissionable nuclides is summarized below:

Fissionable Isotopes in One Canister

	g/lb of glass	g/can.[a]
U-233	4.43E-08	-
U-235	1.96E-02	73
Pu-239	5.61E-02	208
Pu-241	4.46E-03	16
		297

[a]Based on 3,700 lb of glass.

A nuclear criticality safety assessment was made for the DWPF glass melter and for storage of canisters in the interim storage building. The infinite neutron multiplication factor (k_∞) was calculated for two concentrations of Pu-239 and U-235 for the melter and the storage building.

Neutron Multiplication Factor (k_∞)
as a Function of Fissionable Isotopes
in Melter and Interim Storage Building

	Melter		Interim Storage Building	
	Conc 1	Conc 2	Conc 3	Conc 4
Pu-239[a]	1,120	560	280	140
U-235[a]	4,030	2,015	1,000	500
k_∞	0.110	0.063	0.012	0.008

[a] Grams of isotope in 3,650 lbs. of glass

Canister Gamma and Neutron Radiation

Canister radiation as a function of distance for glass containing 5-year-old sludge and precipitate from 15-year-old supernate is described in Table 20. The chemical composition of the glass waste is described in Table 21, the uranium and transuranic radionuclide content in Table 22, and a list of the major contributing isotopes to the gamma dose rate in Table 23.

Table 24 compares calculations of DWPF canister gamma radiation by four different codes and companies. The SRP calculation was made using the "ANISN" and "QAD" codes, the GA Technologies calculation was made using the "PATH" code, the Westinghouse calculation using the "SCAP" and ANISN-W codes, and Bechtel Inc., calculation using GRACE-II. ANISN is a one dimensional discrete ordinate code, the other three codes use point kernal integration techniques. All calculations were made using similar waste glass formulations.

Table 25 compares calculations of DWPF canister neutron radiation by three different methods. Although the calculations differ by a factor of less than 2, the contribution to the total radiation emitted from the canister is only 0.25 - 0.42 rem/hr.

Canister Surface Contamination

The criteria selected for canister surface contamination levels are identical to those specified for Department of Transportation cask shipping limits and are useful guides for canister decontamination by the frit-water slurry blasting technique. Canisters decontaminated to these levels are not expected to significantly contribute to air contamination within the Interim Storage Building. The canister surface contamination limits selected are:

Alpha	220 d/min/100 cm^2
Beta-Gamma	2200 d/min/100 cm^2

Labeling

Each canister will have a letter and four numbers located on the side wall and top head. The letter and numbers will be approximately 2 in. high and will be visible by television viewing. Each number will permit identification of the canister fabrication and processing history.

Canister Temperature

Table 26 describesthe temperature of a canister containing a sludge-precipitate wasteform at power levels of 425 to1000 watts, when in air at temperatures of 20°C and 38°C. Surface temperature of a 690-watt canister is estimated to be 58°C for an air temperature of 38°C. The centerline temperature is estimated to be 89°C for 38°C air temperature.

ESTIMATED PRODUCTION SCHEDULE

The power level and activity of canisters produced in the DWPF as a function of time is dependent on the mixing logistics of sludge, salt, and supernate in the waste tank farm.. In general, the intent is to remove waste from the oldest tanks first, since these tanks also contain the oldest waste. There are, however, practical constraints which limit the flexibility of transfer between areas, as well as between tanks, so that the present sludge inventory is segregated by processing area, somewhat segregated by type (HAW or LAW) and partially segregated by age.

The waste tank sludge and supernate blending schedule continues to be developed and refined. The preliminary schedule was described in "Characteristics of Spent Fuel, High-Level Waste, and Other Radioactive Wastes Which May Require Long-Term Isolation", DOE/RW-0184, December 1987. The data shown in Tables 27 and 28 of this report were developed from the 1988 Integrated Database and updates and the OCRWM December 1987 report. Since the Integrated Database information is developed each year, the schedule will become more accurate as hot startup is approached.

A description of the SRP waste inventory projected to the end of calendar year 1988 is shown in Table 27. At that time, the expected waste volume will be about 127,000 m^3 (33.4 million gallons), contains 778 million curies, and generates 2,300 kilowatts. Contributions of the principal fission product radionuclides are also shown. Of the total, Sr-90/Y-90 and Cs-137/Ba-137 contibute 70% of the total curies.

Table 28 describes the average radioactivity and thermal power per canister of waste glass as a function of time. The table covers the period from 1991 to 2022. Although the table reflects the best estimate of the schedule as of December 1988, it does not necessarily represent the actual processing schedule and tankage allocations; consequently, the data should be updated each year as the radioactive startup date approaches.

REFERENCES

DWPF References

R. G. Baxter, "Design and Construction of the Defense Waste Processing Facility Project at the Savannah River Plant," **Proceedings Waste Management '86, Vol 2**, Tucson, AZ (1986).

K. L. Walker, J. R. White, K. A. Farnstrom, and R. E. Eversole, "Canister Grapple for the Defense Waste Processing Facility." **Proceedings, 34th Conference on Remote Systems Technology** (1986).

Savannah River Plant, **Defense Waste Processing Facility, Basic Data Report**, DPSP-80-1033,E. I. du Pont de Nemours and Company, Savannah River Laboratory, Aiken, SC 29808 (April 1985).

M. D. Boersma, "Process Technology for Vitrification of Defense High-Level Waste at the Savannah River Plant." **ANS-Fuel Reprocessing and Waste Management**, Jackson Hole, WY (August 1984).

Computer Code References

CCC-254, **ANISN-ORNL, A Multigroup One-Dimensional Discrete Ordinance Transport Code with Anisotropic Scattering.** ORNL Radiation Shielding Information Center, Oak Ridge, TN (1983).

CCC-255, **ANISN-W, A One Dimensional Discrete Ordinates Transport Computer Program,** ORNL Radiation Shielding Information Center, Oak Ridge, TN (1971).

CCC-307, **QAD-CG, A Combinatorial Geometry Version of QAD-PSA, A Point Kernal Code for Neutron and Gamma Ray Shielding Calculations,** ORNL Radiation Shielding Information Center, Oak Ridge, TN (1979).

CCC-418, **SCAP, Single Scatter, Albedo Scatter, and Point Kernel Analysis Program in Complex Geometry,** ORNL Radiation Shielding Information Center, Oak Ridge, TN (1982).

Glass Stability Programs

M. J. Plodinec, G. G. Wicks, and N. E. Bibler, " An Assessment of Savannah River Borosilicate Glass in the Repository Environment," USDOE Report DP-1629, E. I. du Pont de Nemours and Co., Savannah River Laboratory, Aiken, SC 29808 (1982).

J. E. Mendel (ed), "Final Report of the Defense High-Level Waste Leaching Program," USDOE Report PNL-5157, Battelle-Pacific Northwest Laboratory, Richland, WA 99352 (1984).

M. J. Plodinec, "Characterization of Savannah River Plant Waste Glass," **Waste Management 85,** 441-5 (1985).

G. G. Wicks, "Nuclear Waste Glasses," **Treatise on Materials Science and Technology, Glass IV,** 57-118 (1985).

G. G. Wicks, "Savannah River Waste Glass Performance," USDOE Report DP-MS-86-35, E. I. du Pont de Nemours and Company, Savannah River Laboratory, Aiken, SC 29808 (1986).

N. E. Bibler, "Glass Performance in a Geologic Setting," USDOE Report DP-MS-86-119, E. I.

du Pont de Nemours and Company, Savannah River Laboratory, Aiken, SC 29808 (1986).

Glass Composition Development

P. D. Soper, D. D. Walker, M. J. Plodinec, G. J. Roberts, and L. F. Lightner, "Optimization of Glass Composition for the Vitrification of Nuclear Waste at the Savannah River Plant," **Bull. Am. Cer. Soc., 62,** 1013-8 (1983).

G. G. Wicks, W. D. Rankin and S. L. Gore, "International Waste Glass Study-Composition and Leachability Correlations," **Scientific Basis for Nuclear Waste Management, VIII,** 171-177 (1985).

M. J. Plodinec, "Vitrification Chemistry and Nuclear Waste," **J. Non-Cryst. Solids, 84,** 206-14 (1986).

C. M. Jantzen, "Systems Approach to Nuclear Waste Glass Development," **J. Non-Cryst. Solids, 84,** 215-25 (1986).

Modeling

R. M. Wallace and G. G. Wicks, "Leaching Chemistry of Defense Borosilicate Glass," **Scientific Basis for Nuclear Waste Management, VI,** 23-29 (1983).

M. J. Plodinec, C. M. Jantzen, and G. G. Wicks, "Thermodynamic Approach to Prediction of the Stability of Proposed Radwaste Glasses," **Advances in Ceramics - Nuclear Waste Management, 8,** 491-95 (1984).

C. M. Jantzen and M. J. Plodinec, "Thermodynamic Model of Natural, Medieval and Nuclear Waste Glass Durability," **J. Non-Cryst. Solids, 67,** 207-23 (1984).

M. J. Plodinec, C. M. Jantzen and G. G. Wicks, "Stability of Radioactive Waste Glasses Assessed from Hydration Thermodynamics," **Scientific Basis for Nuclear Waste Management, VII,** 755-62 (1985).

Long-Term Testing

J. K. Bates, D. J. Lam and M. J. Steindler, "Extended Leach Studies of Actinide-Doped SRL 131 Glass," **Scientific Basis for Nuclear Waste Management, VI,** 183-90 (1983).

G. G. Wicks, G. T. Chandler and R. M. Wallace, "Chemical Durability of SRP Waste Glass - Saturation Effects and Influence of SA/V", USDOE Report DP-MS-84-37, E. I. du Pont de Nemours and Company, Savannah River Laboratory, Aiken, SC 29808 (1984). Available from NTIS, PC A03/MF A01(GPO Dep.).

Waste Glass Saturation Effects and Influence of SA/V

G. G. Wicks, J. A. Stone, G. T. Chandler and S. Williams, **Long Term Behavior of Simulated Savannah River Plant Waste Glass,** USDOE Report DP-1728, E. I. du Pont de Nemours, and Company, Savannah River Laboratory, Aiken, SC 29808 (1986).

Groundwater Eh and pH Effects

C. M. Jantzen, "Effects of Eh (Oxidation Potential) on Borosilicate Waste Glass Durability," **Advances in Ceramics - Nuclear Waste Management, 8,** 385-393 (1984).

C. M. Jantzen, "Methods of Simulating Low Redox Potential (Eh) for a Basalt Repository," **Scientific Basis for Nuclear Waste Management, VII,** 613-621 (1984).

C. M. Jantzen and G. G. Wicks, "Control of Oxidation Potential for Basalt Repository Simulation Tests," **Scientific Basis for Nuclear Waste Management, VIII,** , 29-35 (1985).

C. M. Jantzen and N. E. Bibler, "The Role of Groundwater Oxidation Potential and Radiolysis on Waste Glass Performance in Crystalline Repository Environments," **Scientific Basis for Nuclear Waste Management, IX,** Materials Research Society, Pittsburgh, PA 219-229 (1986).

Effect of Pressure

G. G. Wicks, W. C. Mosley, P. G. Whitkop, and K. A. Saturday, "Durability of Simulated Waste Glass - Effects of Pressure and Formation of Surface Layers," **J. Non-Cryst. Solids, 49,** 413-28 (1982).

Radiation Effects

N. E. Bibler, "Effects of Alpha, Gamma, and Alpha-Recoil Radiation on Borosilicate Glass Containing Savannah River Plant Defense High-Level Nuclear Waste," **Scientific Basis for Nuclear Waste Management, IV,** Elsevier, New York, 681-87 (1982).

J. K. Bates, L. J. Jardine, K. F. Flynn, and M. J. Steindler, "The Application of Neutron Activation Analysis to the Determination of Leach Rates of Simulated Nuclear Waste Forms," USDOE Report ANL-81-34, Argonne National Laboratory, Argonne, IL (February 1982).

G. W. Arnold, C. J. M. Northrup, and N. E. Bibler, "Near-Surface Leaching Studies of Pb-Implanted Savannah River Waste Glass," **Scientific Basis for Nuclear Waste Management, V,** Elsevier, New York, 359-68 (1983).

N. E. Bibler, "Characterization of Borosilicate Glass Containing Savannah River Plant Radioactive Waste," **Glastekn. Ber., 56K,** 736-41 (1983).

J. E. Mendel (ed), "Final Report of the Defense High-Level Waste Leaching Mechanisms Program," USDOE Report PNL-5157, Battelle-Pacific Northwest Laboratory, Richland, WA 99352 (1984).

Devitrification

C. M. Jantzen, D. F. Bickford, D. G. Karraker and G. G. Wicks, "Time-Temperature-Transformation Kinetics in SRL Waste Glass," **Advances in Ceramics - Nuclear Waste Management, 8,** 30-38 (1984).

D. F. Bickford and C. M. Jantzen, "Devitrification Behavior of SRL Defense Waste Glass," **Scientific Basis for Nuclear Waste Management, VII,** Elsevier, New York, 557-66 (1984).

C. M. Jantzen and D. F. Bickford, "Leaching of Devitrified Glass Containing Simulated SRP Nuclear Waste," **Scientific Basis for Nuclear Waste Management, VIII,** Materials Research Society, Pittsburgh, PA, 135-46 (1985).

D. F. Bickford and C. M. Jantzen, "Devitrification of Defense Nuclear Waste Glasses: Role of Melt Insolubles," **J. Non-Cryst. Solids, 84,** 299-307 (1986).

Large-Scale Leach Tests

P. K. Smith, and C. A. Baxter, "Fracture During Cooling of Cast Borosilicate Glass Containing Nuclear Wastes," USDOE Report DP-1602, E. I. du Pont de Nemours & Co., Savannah River Laboratory, Aiken, SC (1981).

D. J. Pellarin and D. F. Bickford, **Large Scale Leach Test Facility: Development of Equipment and Methods, and comparison to MCC-1,** USDOE Report DPST-85-615, E. I. du Pont de Nemours and Company, Savannah River Laboratory, Aiken, SC 29808 (1985).

D. F. Bickford and D. J. Pellarin, "Large Scale Leach Testing of DWPF Canister Sections," **Scientific Basis for Nuclear Waste Management, X** (1987).

Interactions with Package Components

G. G. Wicks, B. M. Robnett and W. D. Rankin, "Chemical Durability of Glass Containing SRP Waste-Leachability Characteristics, Protective Layer Formation, and Repository Systems Interactions," **Scientific Basis for Nuclear Waste Management, V** 15-24 (1982).

D. B. Burns, B. H. Upton and G. G. Wicks, "Interactions of SRP Waste Glass with Potential Canisters and Overpack Metals," **J. Non-Cryst. Solids, 84,** 258-267 (1986).

In-Situ Tests

D. E. Clark, B. F. Zhu, L. L. Hench, G. G. Wicks and L. O. Werme, "An Evaluation of Six-Month Burial Data from Stripa," **Rivista della Staz. Sper. Vetro., 5,** 185-95 (1984).

D. E. Clark, B. F. Zhu, R. S. Robinson and G. G. Wicks, "Preliminary Report on a Glass Burial Experiment in Granite," **Advances in Ceramics - Nuclear Waste Management, 8,** 324-36 (1984).

A. Lodding, D. E. Clark, L. O. Werme, and G. G. Wicks, "SRL Glasses Leached in a Burial Environment: SIMS Study of Element Distributions," Proceeding of the 1984 International Symposium on Glass, in Beijing.

D. E. Clark, B. F. Zhu and G. G. Wicks, "Nuclear Waste Glass Leaching-Comparison of Laboratory and Field Tests," Proceeding of the 1984 International Symposium on Glass, in Beijing.

B. F. Zhu, D. E. Clark, L. L. Hench, G. G. Wicks and L. O. Werme, "One-Year Leaching of Three SRL Glasses in Granite," **Scientific Basis for Nuclear Waste Management, VIII,** 187-194 (1985).

G. G. Wicks, **WIPP/SRL In-Situ and Lab Testing Programs-Part I: MIIT Overview, Nonradioactive Waste Glass Studies,** USDOE Report DP-1706, E. I. du Pont de Nemours and Company, Savannah River Laboratory, Aiken SC 29808 (1986).

G. G. Wicks, M. E. Weinle, and M. A. Molecke, "WIPP/SRL In-Situ Tests-Part II: Pictorial History of MIIT and Final MIIT Matrices, Assemblies, and Sample Listings," USDOE Report DP-1733, E. I. du Pont de Nemours and Company, Savannah River Laboratory, Aiken, SC 29808 (1987).

B. F. Zhu, D. E. Clark, A. Lodding, and G. G. Wicks, "Two-Year Leaching Behavior of Three SRL Nuclear Waste Glasses in Granite." **Advances in Ceramics, 20** 1987.

A. Lodding, E. U. Engström, D. E. Clark, L. O. Werme and G. G. Wicks, "SIMS Analysis of Leached Layers Formed on SRL Glasses During Burial." **Advances in Ceramics, 20** 1987.

G. G. Wicks, M. E. Weinle, and M. A. Molecke, "WIPP/SRL In-Situ Tests - Part II: Pictorial History of MIIT and Final MIIT Matrices, Assemblies, and Sample Listings," USDOE Report DP-1733, E. I. du Pont de Nemours and Company, Savannah River Laboratory, Aiken, SC 29808 (1987).

Repository Simulation Tests

G. G. Wicks, N. E. Bibler, C. M. Jantzen and M. J. Plodinec, "Repository Simulation Tests." E. I. du Pont de Nemours and Company, Savannah River Laboratory, Aiken, SC 29808 (1984). Available from NTIS PC A02/MF A01 (GPO Dep.).

J. E. Mendel (ed.), "Final Report of the Defense High-Level Waste Leaching Mechanisms Program," USDOE Report PNL-5157, Battelle-Pacific Northwest Laboratory, Richland, WA 99352 (1984).

N. E. Bibler, G. G. Wicks and V. O. Oversby, "Leaching of SRP Nuclear Waste Glass in a Saturated Tuff Environment," **Scientific Basis for Nuclear Waste Management, VIII,** 247-56 (1985).

G. G. Wicks, "Nuclear Waste Vitrification - The Geology Connection," **J. Non-Cryst. Solids, 84,** 241-50 (1986).

N. E. Bibler, M. J. Plodinec, G. G. Wicks and C. M. Jantzen, **"Glass Performance in a Geologic Setting."** USDOE Report DP-MS-86-119, E. I. du Pont de Nemours and Company, Savannah River Laboratory, Aiken, SC 29808 (1986).

N. E. Bibler and C. M. Jantzen, "Materials Interactions Relating to Long-Term Geologic Disposal of Nuclear Waste Glass," **Scientific Basis for Nuclear Waste Management, X**(1987).

W. D. Rankin and G. G. Wicks, "Chemical Durability of SRP Waste Glass as a Function of Waste Loading." **J. Am. Cer. Soc., 66,** 417-420 (1983).

B. F. Zhu, D. E. Clark, L. L. Hench, and G. G. Wicks, "Leaching Behavior of Nuclear Waste Glass Heterogeneities." **J. Non-Cryst. Solids, 80,** 324-34 (1986).

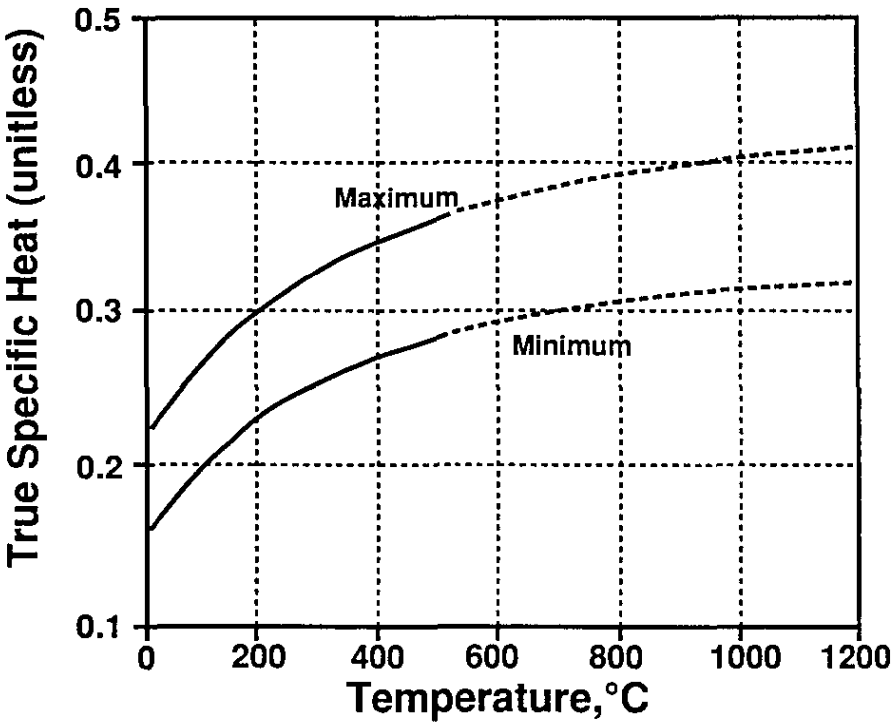

Figure 1. Calculated True Specific Heat of DWPF Glass

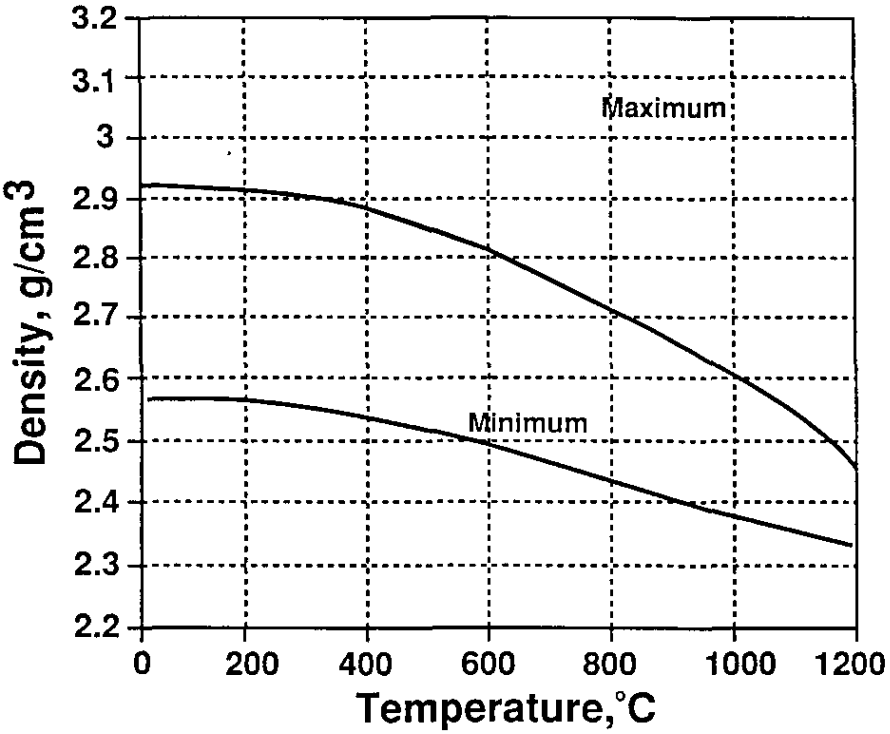

Figure 2. Calculated Density of DWPF Glass

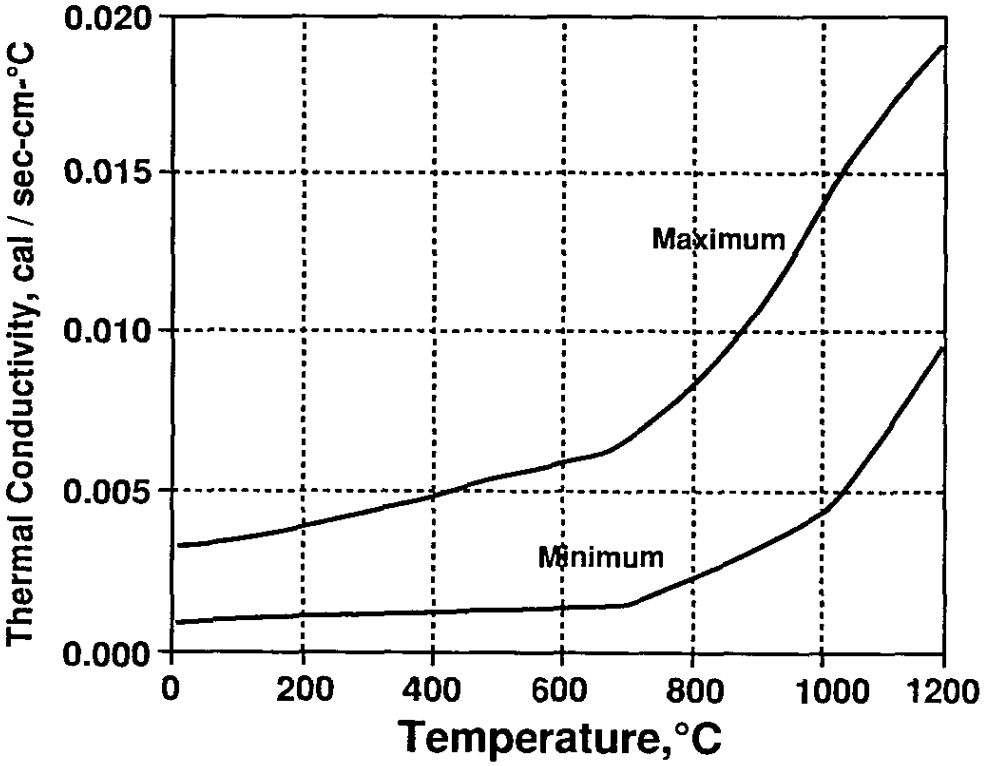

Figure 3. Calculated Thermal Conductivity of DWPF Glass

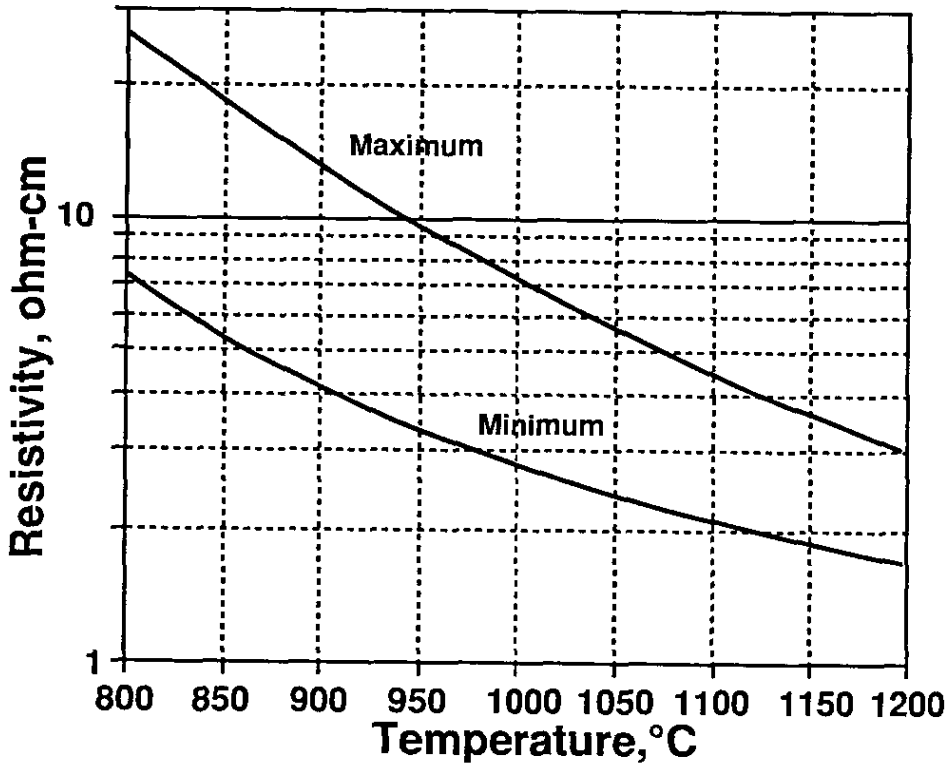

Figure 4. Experimental Resistivity of DWPF Glass

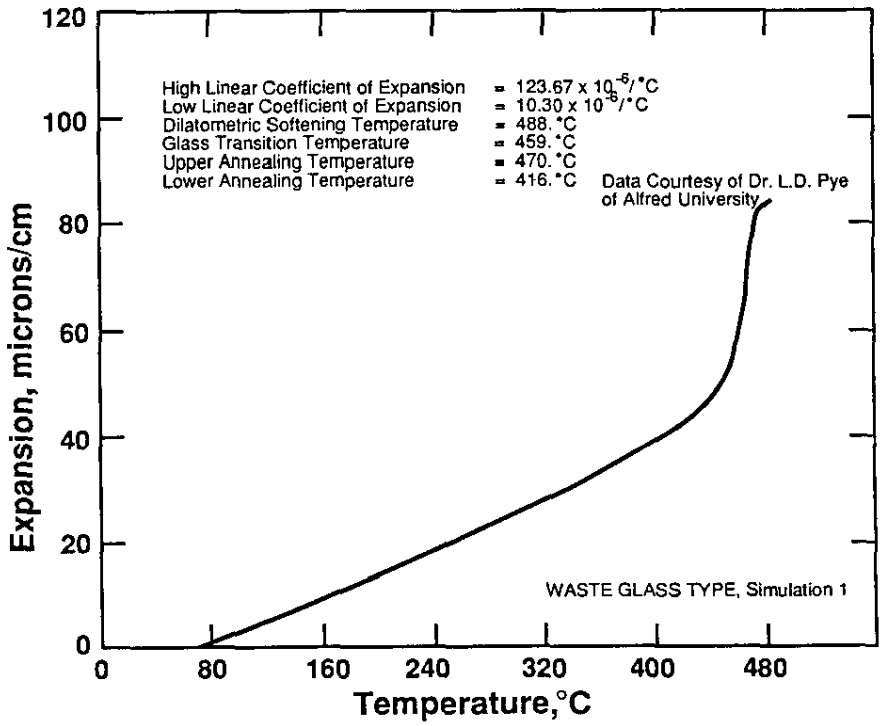

Figure 5. Experimental Thermal Expansion Data for Simulated Waste Glass, Simulation 1

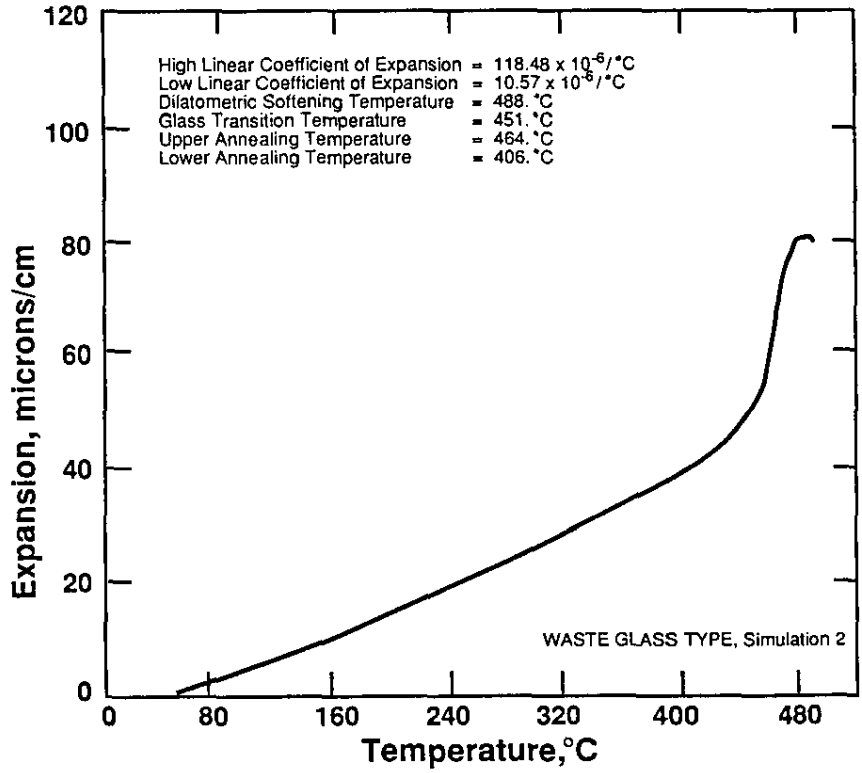

Figure 6. Experimental Thermal Expansion Data for Simulated Waste Glass, Simulation 2

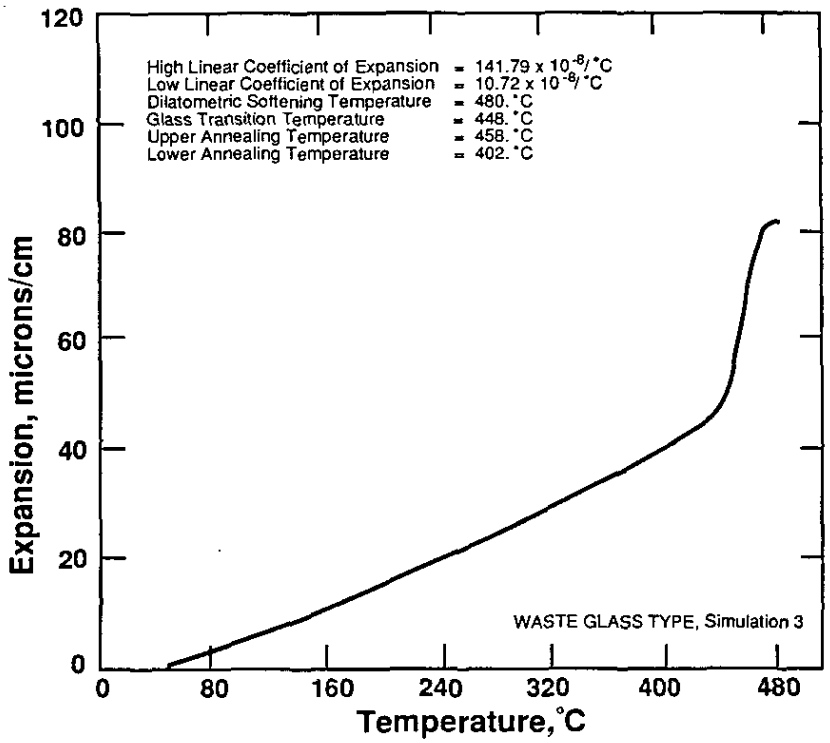

Figure 7. Experimental Thermal Expansion Data for Simulated Waste Glass, Simulation 3

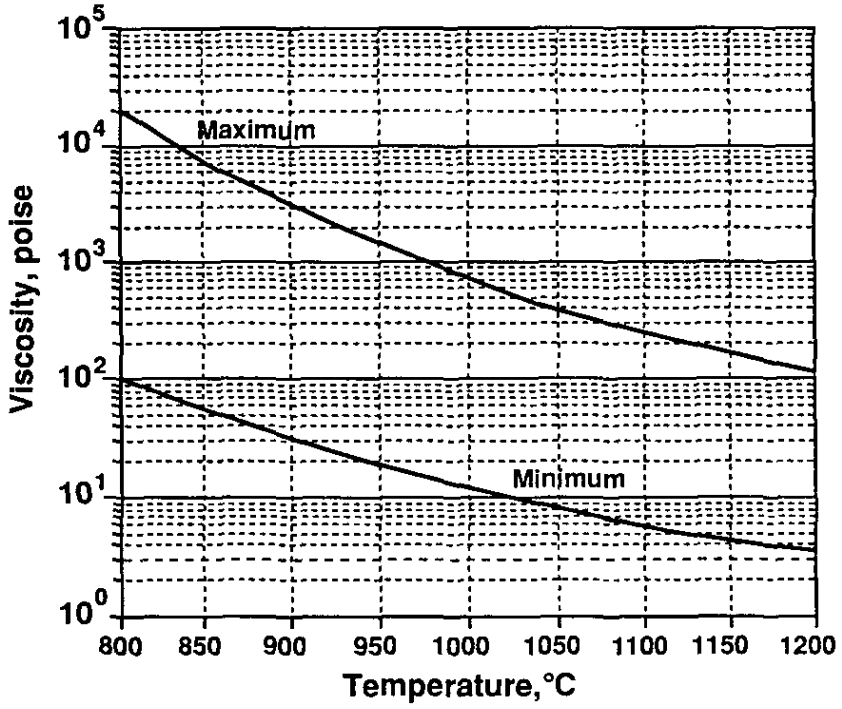

Figure 8. Experimental Viscosity of DWPF Glass

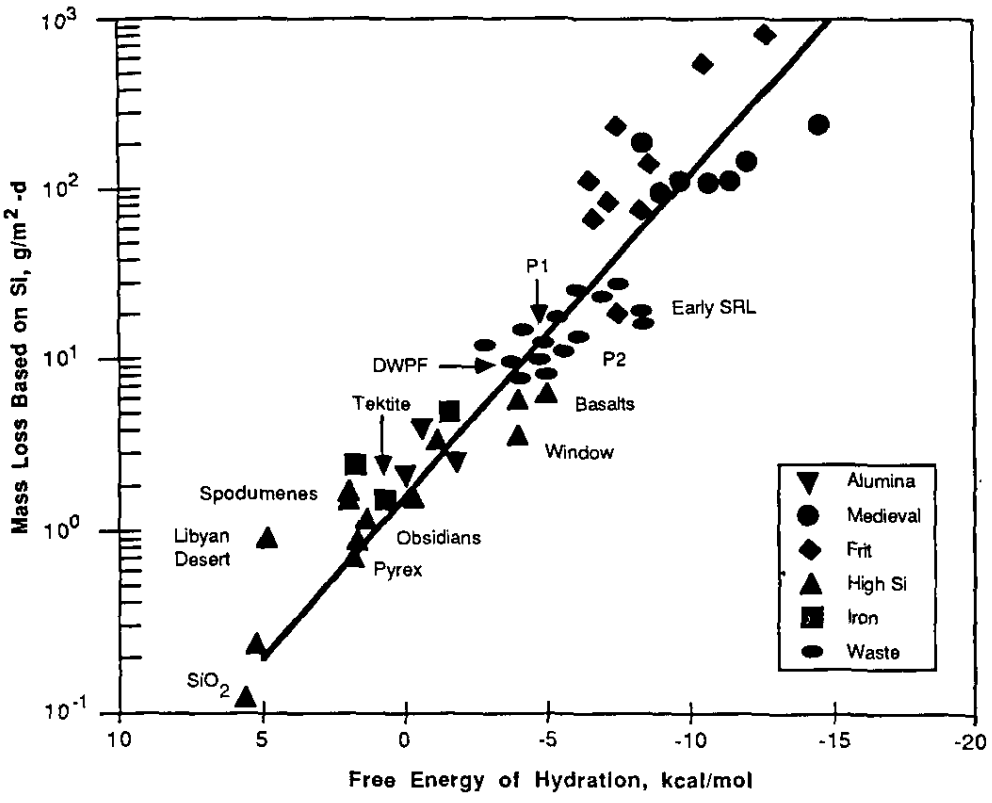

M812178

Figure 9. Durability of Glasses and Minerals in an MCC-1 Leach Test. Glasses were Exposed for 28 Days in 90°C Deionized Water.

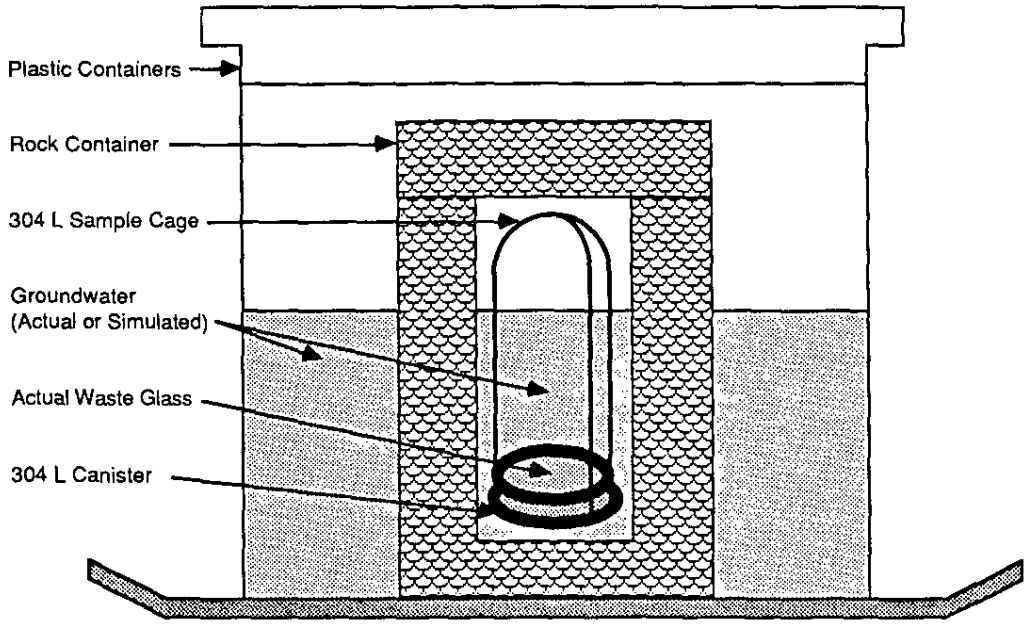

M812178

Figure 10. Repository Simulation Test Vessels

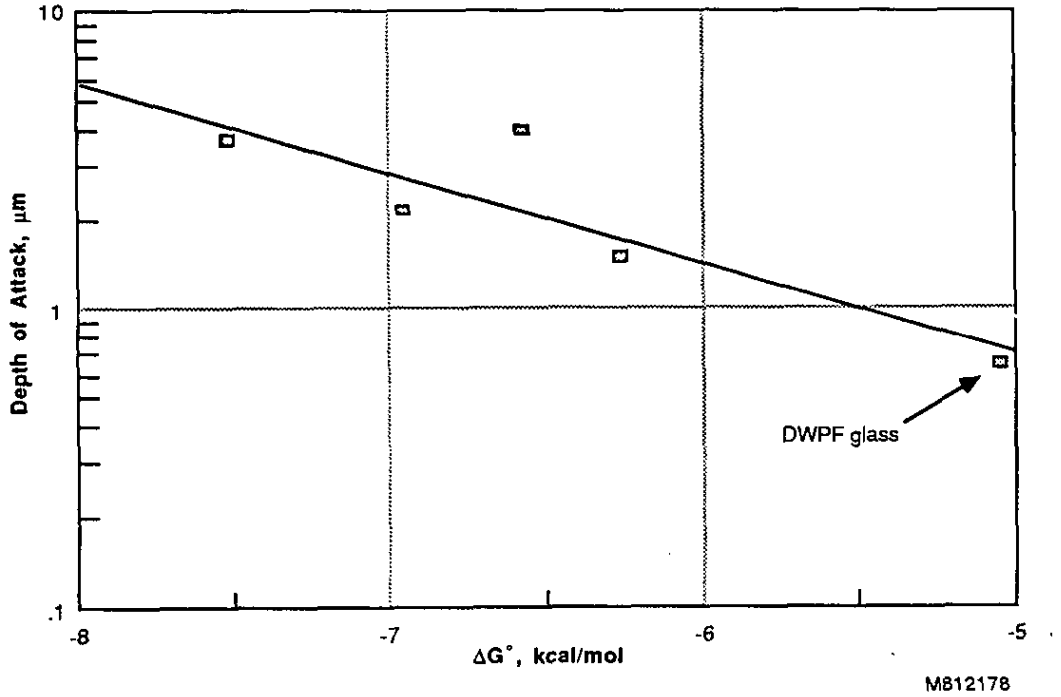

Figure 11. Results from 2-Year Burial Experiments

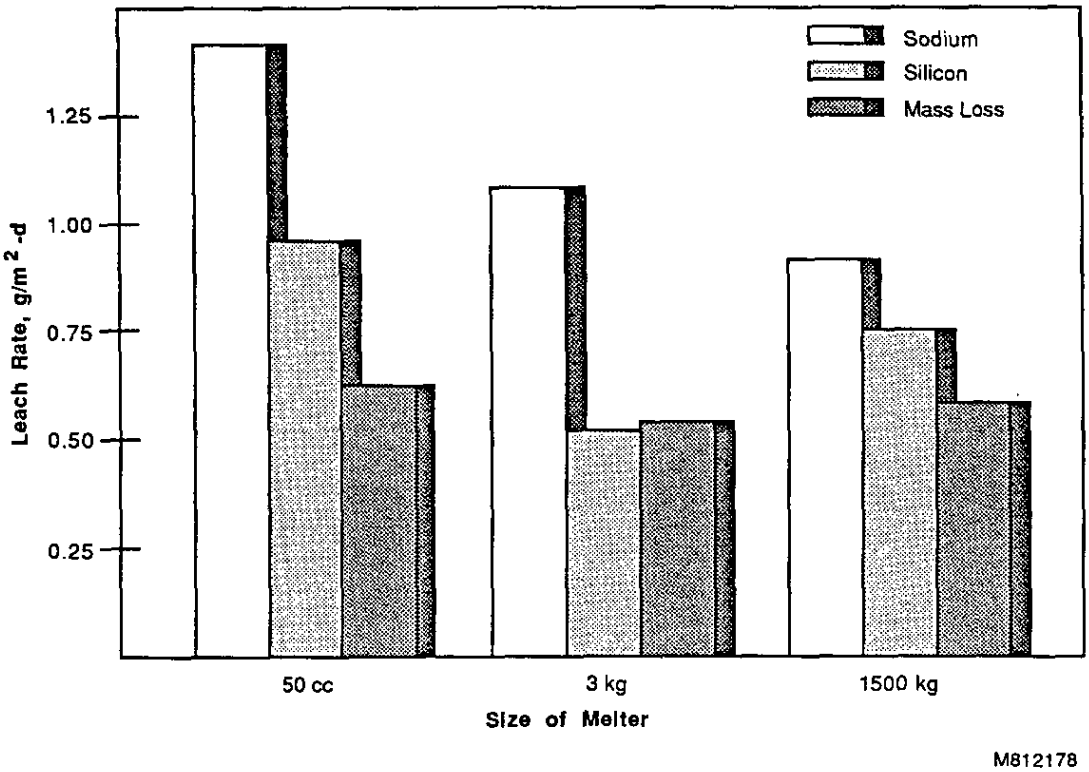

Figure 12. Effect of Melter Size on Glass Leaching

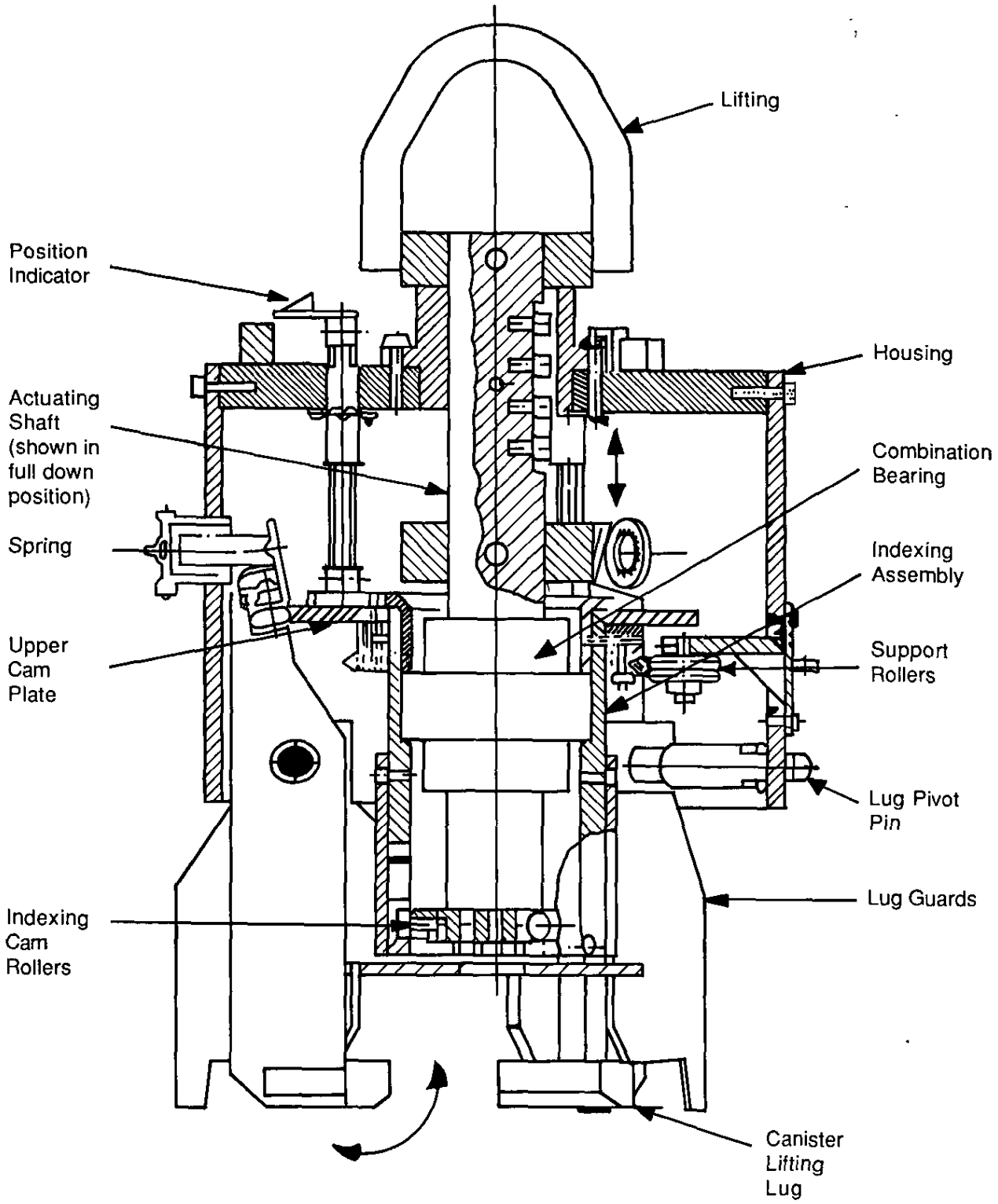

Figure 13. Canister Grapple

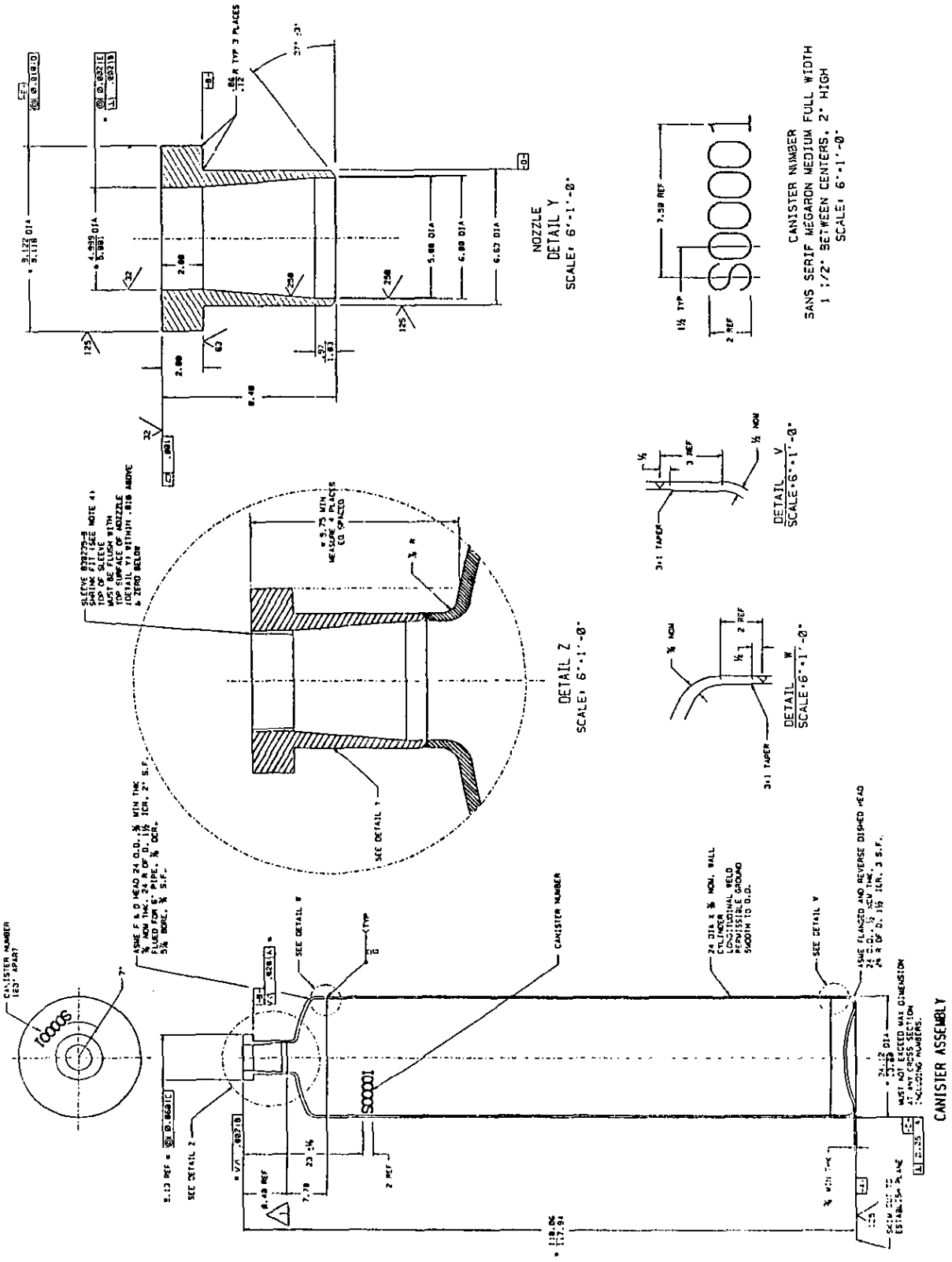

Figure 14. Canister Assembly

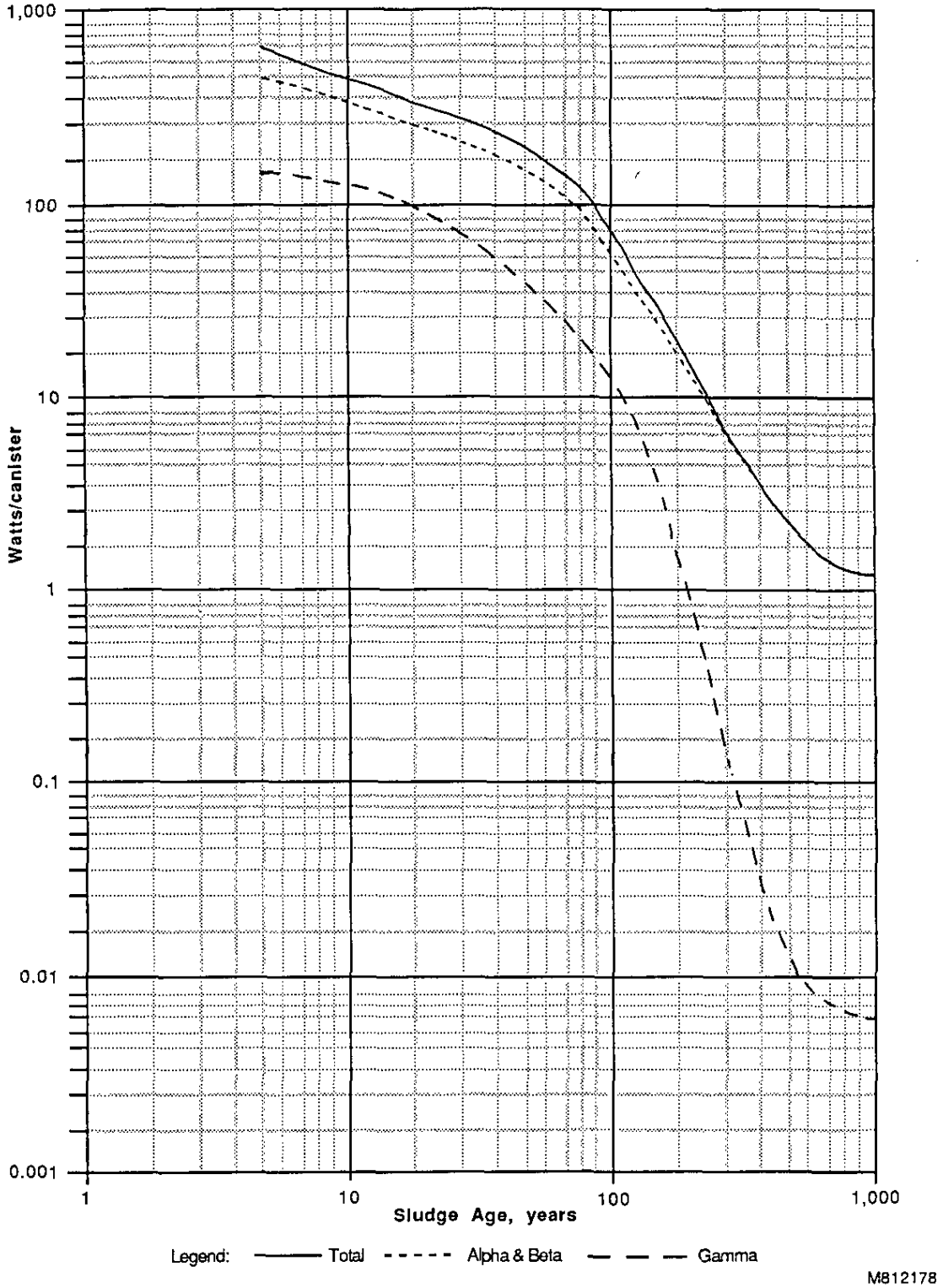

Figure 15. Sludge-Precipitate Canister Decay Heat

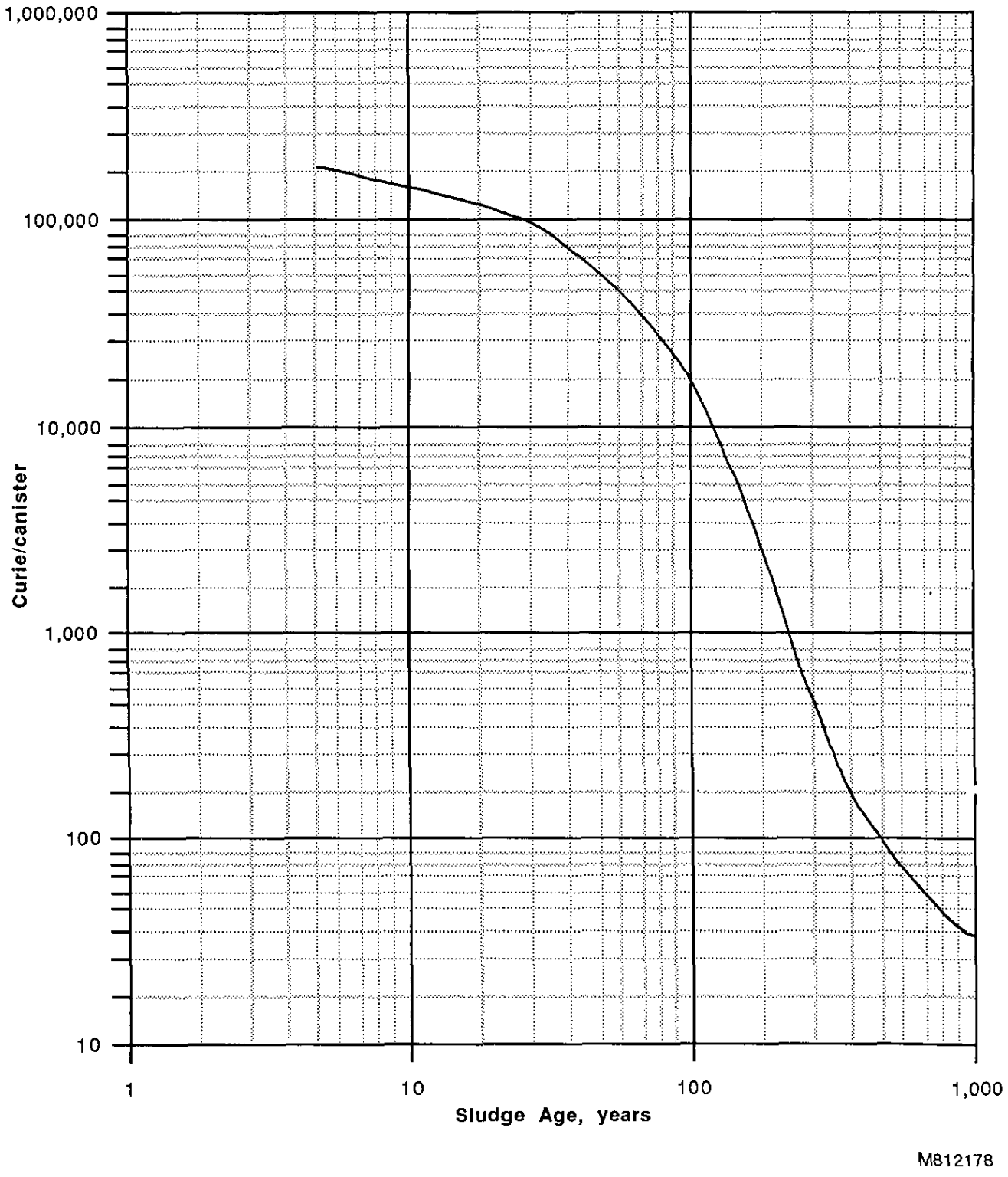

Figure 16. Sludge-Precipitate Canister Activity

Table 1A

Chemical Composition of Sludge Feed Soluble Solids (Dry Basis)

Component	wt%	Component	wt%
$Ba(NO_3)_2$	0.649E-02	Na_2SO_4	0.492E+01
$CaSO_4$	0.642E-03	NA_2SiO_3	0.116
$CsNO_3$	0.716E-02	NA_3PO_4	0.349
Group A[a]	0.390E-02	$NaAg(OH)_2$	0.191E-03
KNO_3	0.500	$NaAl(OH)_4$	0.107E+02
NH_4NO_3	0.199E-01	NaCl	0.307
Na[(HgO)(OH)]	0.829E-02	NaF	0.154
$Na_2C_2O_4$	0.267	NaI	0.372E-03
Na_2CO_3	0.432E+01	$NaNO_2$	0.194E+02
Na_2CrO_4	0.133	$NaNO_3$	0.406E+02
Na_2MoO_4	0.219E-01	NaOH	0.182E+02
Na_2RhO_4	0.552E-03	$UO_2(OH)_2$	0.302E-04
Na_2RuO_4	0.237E-02		

[a] Cd, Mo, Rb, Se, Tc, and Te.

Table 1B

Chemical Composition of Sludge Feed Insoluble Solids (Dry Basis)

Component	wt%	Component	wt%
AgOH	0.168	Na_2SO_4	0.132
$Al(OH)_3$	0.157E+02	Na_3PO_4	0.121E-01
$BaSO_4$	0.386	NaCl	0.110E+01
$Ca_3(PO_4)_2$	0.189	NaF	0.965E-01
CaC_2O_4	0.878	NaI	0.161E-01
$CaCO_3$	0.346E+01	$NaNO_3$	0.232E+01
CaF_2	0.151	NaOH	0.403E+01
$CaSO_4$	0.281	$Ni(OH)_2$	0.320E+01
Carbon	0.125	$PbCO_3$	0.114
$Co(OH)_3$	0.109E-01	$PbSO_4$	0.280
$Cr(OH)_3$	0.443	Pd(OH)2	0.622E-01
$CsNO_3$	0.124E-01	PuO_2	0.577E-01
$Cu(OH)_2$	0.159	RhO_2	0.262E-01
$Fe(OH)_3$	0.405E+02	RuO_2	0.134
Group A[a]	0.240	SiO_2	0.308E+01
Group B[b]	0.104E+01	$SrCO_3$	0.177
HgO	0.141E+01	ThO_2	0.567
KNO_3	0.536	$UO_2(OH)_2$	0.673E+01
$Mg(OH)_2$	0.400	$Y_2(CO_3)_3$	0.688E-01
MnO_2	0.691E+01	Zeolite	0.453E+01
		$Zn(OH)_2$	0.270

[a] Cd, Mo, Rb, Se, Tc, and Te.

[b] Ag, Am, Ce, Cm, Co, Cr, Eu, La, Nb, Nd, Np, Pm, Pr, Sb, Sm, Sn, Tb, Tl, and Zr.

Table 2

Radionuclide Content of Sludge Feed

Isotope	Ci/Gal	Isotope	Ci/Gal	Isotope	Ci/Gal
H-3	1.93E-05	Sb-126m	1.28E-04	Eu-154	5.48E-01
C-14	3.21E-08	Te-125m	2.56E-01	Eu-155	4.21E-01
Cr-51	8.24E-20	Te-127	1.12E-04	Eu-156	4.64E-35
Co-60	1.50E-01	Te-127m	1.14E-04	Tb-160	9.91E-10
Ni-59	2.08E-05	Te-129	2.84E-15	Tl-208	9.70E-07
Ni-63	2.58E-03	Te-129m	4.44E-15	U-232	1.17E-05
Se-79	1.58E-04	I-129	1.31E-08	U-233	1.38E-09
Rb-87	5.55E-10	Cs-134	1.41E-01	U-234	2.98E-05
Sr-89	3.72E-08	Cs-135	2.47E-06	U-235	1.37E-07
Sr-90	4.05E+01	Cs-136	4.26E-43	U-236	9.80E-07
Y-90	4.16E+01	Cs-137	1.34E+00	U-238	9.14E-06
Y-91	6.57E-07	Ba-136m	7.52E-42	Np-236	1.52E-11
Zr-93	9.90E-04	Ba-137m	1.28E+00	Np-237	7.74E-06
Zr-95	8.90E-06	Ba-140	8.95E-40	Pu-236	1.07E-04
Nb-94	8.39E-08	La-140	3.83E-40	Pu-237	7.81E-15
Nb-95	1.89E-05	Ce-141	3.18E-14	Pu-238	1.30E+00
Nb-95m	1.10E-07	Ce-142	8.45E-09	Pu-239	1.13E-02
Tc-99	2.78E-03	Ce-144	8.74E+00	Pu-240	7.59E-03
Ru-103	1.50E-11	Pr-143	1.06E-37	Pu-241	1.46E+00
Ru-106	2.00E+00	Pr-144	8.74E+00	Pu-242	1.07E-05
Rh-103m	1.46E-11	Pr-144m	1.04E-01	Am-241	9.47E-03
Rh-106	2.01E+00	Nd-144	4.27E-13	Am-242	1.26E-05
Pd-107	1.27E-05	Nd-147	1.12E-47	Am-242m	1.26E-05
Ag-110m	1.10E-04	Pm-147	2.14E+01	Am-243	5.06E-06
Cd-113	4.64E-17	Pm-148	6.16E-14	Cm-242	3.09E-05
Cd-115m	1.13E-12	Pm-148m	8.93E-13	Cm-243	4.88E-06
Sn-121m	2.54E-05	Sm-147	1.73E-09	Cm-244	9.40E-02
Sn-123	2.26E-04	Sm-148	5.02E-15	Cm-245	5.84E-09
Sn-126	1.29E-04	Sm-149	1.55E-15	Cm-246	4.66E-10
Sb-124	6.31E-11	Sm-151	2.16E-01	Cm-247	5.72E-16
Sb-125	7.34E-01	Eu-152	3.26E-03	Cm-248	5.98E-16
Sb-126	1.80E-05				

Total actvity	1.33E+02 Ci/Gal
Decay heat	
Total primary	4.21E-01 Watt/Gal
Total gammas	1.92E-02 Watt/Gal

Table 3

Partial Isotopic Content of Sludge Feed

Isotope	G/Gal	Isotope	G/Gal	Isotope	G/Gal
H-3	2.01E-09	Ru-104	7.21E-02	Te-125	2.86E-03
C-14	7.21E-09	Ru-106	5.98E-04	Te-125m	1.42E-05
Cr-51	8.92E-25	Rh-103	7.52E-02	Te-126	1.25E-04
Co-60	1.33E-04	Rh-103m	4.48E-19	Te-127	4.23E-11
Ni-59	2.57E-04	Rh-106	5.64E-10	Te-127m	1.21E-08
Ni-63	4.37E-05	Pd-104	9.85E-03	Te-128	3.41E-02
Se-77	3.66E-04	Pd-105	7.85E-02	Te-129	1.36E-22
Se-78	9.19E-04	Pd-106	5.06E-02	Te-129m	1.47E-19
Se-79	2.26E-03	Pd-107	2.46E-02	Te-130	1.23E-01
Se-80	5.40E-03	Pd-108	1.45E-02	I-127	1.99E-05
Se-82	1.09E-02	Pd-110	5.04E-03	I-129	7.40E-05
Rb-85	2.58E-03	Ag-109	5.13E-03	Cs-133	1.69E-02
Rb-87	6.34E-03	Ag-110m	2.32E-08	Cs-134	1.09E-04
Sr-88	2.02E-01	Cd-110	6.18E-04	Cs-135	2.14E-03
Sr-89	1.28E-12	Cd-111	2.91E-03	Cs-136	5.75E-48
Sr-90	2.97E-01	Cd-112	2.01E-03	Cs-137	1.54E-02
Y-89	1.37E-01	Cd-113	1.36E-04	Ba-134	2.89E-02
Y-90	7.65E-05	Cd-114	3.26E-03	Ba-136	3.06E-03
Y-91	2.68E-11	Cd-115m	4.42E-17	Ba-136m	2.77E-53
Zr-90	2.78E-02	Cd-116	1.51E-03	Ba-137	1.18E-01
Zr-91	2.21E-01	Sn-116	2.09E-04	Ba-137m	2.38E-09
Zr-92	2.27E-01	Sn-117	1.08E-03	Ba-138	1.05E+00
Zr-93	3.93E-01	Sn-118	1.16E-03	Ba-140	1.23E-44
Zr-94	2.51E-01	Sn-119	1.13E-03	La-139	3.80E-01
Zr-95	4.15E-10	Sn-120	1.17E-03	La-140	6.88E-46
Zr-96	2.52E-01	Sn-121m	4.72E-07	Ce-140	3.74E-01
Nb-94	4.48E-07	Sn-122	1.31E-03	Ce-141	1.12E-18
Nb-95	4.81E-10	Sn-123	2.75E-08	Ce-142	3.52E-01
Nb-95m	2.90E-13	Sn-124	1.96E-03	Ce-144	2.74E-03
Mo-95	2.52E-01	Sn-125	1.58E-61	Pr-141	3.51E-01
Mo-96	1.02E-03	Sn-126	4.54E-03	Pr-143	1.58E-42
Mo-97	2.40E-01	Sb-121	1.26E-03	Pr-144	1.16E-07
Mo-98	2.48E-01	Sb-123	1.59E-03	Pr-144m	5.76E-10
Mo-100	2.65E-01	Sb-124	3.60E-15	Nd-142	1.25E-03
Tc-99	1.64E-01	Sb-125	7.11E-04	Nd-143	4.19E-01
Ru-100	1.67E-03	Sb-126	2.15E-10	Nd-144	3.60E-01
Ru-101	1.94E-01	Sb-126m	1.63E-12	Nd-145	2.32E-01
Ru-102	1.43E-01	Te-122	2.69E-05	Nd-146	1.88E-01
Ru-103	4.65E-16	Te-124	1.25E-05	Nd-147	1.39E-52
Nd-148	1.09E-01	Eu-156	8.41E-40	Pu-238	7.57E-02
Nd-150	4.35E-02	Tb-159	1.81E-04	Pu-239	1.82E-01
Pm-147	2.31E-02	Tb-160	8.77E-14	Pu-240	3.34E-02
Pm-148	3.75E-19	Tl-206	1.99E-29	Pu-241	1.44E-02

Table 3 Contd

Partial Isotopic Content of Sludge Feed

Isotope	G/Gal	Isotope	G/Gal	Isotope	G/Gal
Pm-148m	4.18E-17	Tl-207	3.28E-19	Pu-242	2.73E-03
Sm-147	7.42E-02	Tl-208	3.29E-15	Am-241	2.76E-03
Sm-148	1.65E-02	Tl-209	9.63E-24	Am-242	1.55E-11
Sm-149	6.43E-03	U-232	5.42E-07	Am-242m	1.30E-06
Sm-150	9.13E-02	U-233	1.43E-07	Am-243	2.54E-05
Sm-151	8.19E-03	U-234	4.77E-03	Cm-242	9.32E-09
Sm-152	3.29E-02	U-235	6.33E-02	Cm-243	9.46E-08
Sm-154	5.85E-03	U-236	1.51E-02	Cm-244	1.16E-03
Eu-151	3.43E-04	U-238	2.72E+01	Cm-245	3.39E-08
Eu-152	1.84E-05	Np-236	1.16E-09	Cm-246	1.52E-09
Eu-153	1.81E-02	Np-237	1.10E-02	Cm-247	6.17E-12
Eu-154	2.03E-03	Pu-236	2.01E-07	Cm-248	1.41E-13
Eu-155	9.04E-04	Pu-237	6.47E-19		
	Total	3.60E+01 G/Gal			

Table 4

Chemical Composition of Precipitate Feed from In-Tank Processing to Salt Cell

Component	Water Free wt%
$Al(OH)_3$	0.47
CsTPB	0.79
$Fe(OH)_3$	0.49
$Hg(C_6H_5)_2$	0.88
KTPB	75.60
NH_4TPB	3.54
$Na_2C_2O_4$	0.97
Na_2CO_3	0.62
Na_2SO_4	0.71
$NaAl(OH)_4$	1.31
$NaNO_2$	1.48
$NaNO_3$	5.96
NAOH	2.40
NaTBP	0.66
$NaTi_2O_5H$	3.52
Others	0.60
Total	100.00

Table 5

Radionuclide Content of Precipitate Slurry Feed to the Salt Cell

Isotope	Ci/Gal	Isotope	Ci/Gal	Isotope	Ci/Gal
H-3	9.06E-05	Sb-124	8.88E-30	Tb-160	2.64E-27
C-14	1.98E-09	Sb-125	1.50E-02	Tl-208	2.67E-08
Co-60	3.28E-04	Sb-126	3.22E-05	U-232	1.67E-07
Ni-59	2.25E-07	Sb-126m	2.30E-04	U-233	2.45E-11
Ni-63	2.72E-05	Te-125m	2.15E-07	U-234	8.35E-07
Se-79	3.75E-07	Te-127	9.73E-20	U-235	1.48E-09
Rb-87	2.25E-10	Te-127m	9.94E-20	U-236	1.07E-08
Sr-89	7.92E-32	I-129	1.51E-10	U-238	9.91E-08
Sr-90	3.99E-01	Cs-134	1.66E-01	Np-236	1.96E-13
Y-90	4.12E-01	Cs-135	8.37E-05	Np-237	1.00E-07
Y-91	4.93E-28	Cs-137	3.60E+01	Pu-236	1.20E-07
Zr-93	4.08E-07	Ba-137m	3.44E+01	Pu-237	8.04E-41
Zr-95	6.26E-26	Ce-141	2.17E-50	Pu-238	1.53E-02
Nb-94	9.10E-10	Ce-142	3.63E-11	Pu-239	1.44E-04
Nb-95	1.32E-25	Ce-144	5.11E-06	Pu-240	9.71E-05
Nb-95m	7.74E-28	Pr-144	5.13E-06	Pu-241	1.16E-02
Tc-99	6.97E-05	Pr-144m	6.13E-08	Pu-242	1.37E-07
Ru-103	3.85E-41	Nd-144	1.85E-15	Am-241	2.40E-04
Ru-106	3.14E-05	Pm-147	6.56E-03	Am-242	1.55E-07
Rh-103m	3.75E-41	Pm-148	6.31E-43	Am-242m	1.56E-07
Rh-106	3.15E-05	Pm-148m	9.16E-42	Am-243	6.52E-08
Pd-107	1.38E-07	Sm-147	3.35E-11	Cm-242	1.28E-07
Ag-110m	3.18E-10	Sm-148	7.56E-17	Cm-243	4.94E-08
Cd-113	5.23E-20	Sm-149	2.32E-17	Cm-244	1.20E-03
Cd-115m	2.81E-40	Sm-151	3.02E-03	Cm-245	7.53E-11
Sn-121m	3.93E-05	Eu-152	1.07E-05	Cm-246	6.00E-12
Sn-123	1.21E-12	Eu-154	1.37E-03	Cm-247	7.38E-18
Sn-126	2.30E-04	Eu-155	5.54E-04	Cm-248	7.73E-18

Total activity	7.14E+01 Ci/Gal
Decay heat	
Total primary	4.33E-02 Watt/Gal
Total gammas	1.24E-01 Watt/Gal

Table 6

Partial Isotopic Content of Precipitate Slurry Feed to the Salt Cell

Isotope	G/Gal	Isotope	G/Gal	Isotope	G/Gal
H-3	9.43E-09	Ru-106	9.38E-09	Te-126	1.33E-09
C-14	4.44E-10	Rh-103	9.90E-04	Te-127	3.68E-26
Co-60	2.90E-07	Rh-103m	1.15E-48	Te-127m	1.05E-23
Ni-59	2.79E-06	Rh-106	8.85E-15	Te-128	3.63E-07
Ni-63	4.61E-07	Pd-104	1.07E-04	Te-129	1.74E-60
Se-77	8.63E-07	Pd-105	8.53E-04	Te-129m	1.88E-57
Se-78	2.18E-06	Pd-106	5.62E-04	Te-130	1.31E-06
Se-79	5.37E-06	Pd-107	2.68E-04	I-127	2.31E-07
Se-80	1.28E-05	Pd-108	1.58E-04	I-129	8.56E-07
Se-82	2.58E-05	Pd-110	5.50E-05	Cs-133	5.76E-01
Rb-85	1.04E-03	Ag-109	1.03E-02	Cs-134	1.28E-04
Rb-87	2.57E-03	Ag-110m	6.68E-14	Cs-135	7.26E-02
Sr-88	2.54E-03	Cd-110	6.93E-07	Cs-137	4.15E-01
Sr-89	2.72E-36	Cd-111	3.26E-06	Ba-134	3.82E-04
Sr-90	2.92E-03	Cd-112	2.25E-06	Ba-136	3.38E-05
Y-89	1.49E-03	Cd-113	1.54E-07	Ba-137	3.23E-03
Y-90	7.57E-07	Cd-114	3.67E-06	Ba-137m	6.39E-08
Y-91	2.01E-32	Cd-115m	1.10E-44	Ba-138	1.15E-02
Zr-90	2.85E-05	Cd-116	1.69E-06	Ce-140	1.61E-03
Zr-91	9.12E-05	Sn-116	3.74E-04	Ce-141	7.61E-55
Zr-92	9.36E-05	Sn-117	1.94E-03	Ce-142	1.51E-03
Zr-93	1.62E-04	Sn-118	2.08E-03	Ce-144	1.60E-09
Zr-94	1.04E-04	Sn-119	2.02E-03	Pr-141	1.51E-03
Zr-95	2.92E-30	Sn-120	2.10E-03	Pr-144	6.78E-14
Zr-96	1.08E-04	Sn-121m	7.32E-07	Pr-144m	3.38E-16
Nb-94	4.85E-09	Sn-122	2.34E-03	Nd-142	5.37E-06
Nb-95	3.36E-30	Sn-123	1.47E-16	Nd-143	1.80E-03
Nb-95m	2.04E-33	Sn-124	3.51E-03	Nd-144	1.56E-03
Mo-95	2.30E-03	Sn-126	8.10E-03	Nd-145	9.95E-04
Mo-96	9.33E-06	Sb-121	3.27E-04	Nd-146	8.10E-04
Mo-97	2.20E-03	Sb-123	4.13E-04	Nd-148	4.67E-04
Mo-98	2.26E-03	Sb-124	5.07E-34	Nd-150	1.87E-04
Mo-100	2.42E-03	Sb-125	1.45E-05	Pm-147	7.07E-06
Tc-99	4.11E-03	Sb-126	3.85E-10	Pm-148	3.84E-48
Ru-100	2.50E-05	Sb-126m	2.93E-12	Pm-148m	4.28E-46
Ru-101	1.93E-03	Te-122	2.87E-10	Sm-147	1.44E-03
Ru-102	2.13E-03	Te-124	1.34E-10	Sm-148	2.48E-04
Ru-103	1.19E-45	Te-125	4.04E-08	Sm-149	9.66E-05
Ru-104	1.07E-03	Te-125m	1.19E-11	Sm-150	1.37E-03
Sm-151	1.15E-04	U-232	7.78E-09	Pu-241	1.15E-04
Sm-152	4.93E-04	U-233	2.54E-09	Pu-242	3.49E-05
Sm-154	8.78E-05	U-234	1.34E-04	Am-241	6.98E-05
Eu-151	5.22E-06	U-235	6.86E-04	Am-242	1.91E-13
Eu-152	6.05E-08	U-236	1.65E-04	Am-242m	1.60E-08

Table 6 Contd

Partial Isotopic Content of Precipitate Slurry Feed to the Salt Cell

Isotope	G/Gal	Isotope	G/Gal	Isotope	G/Gal
Eu-153	1.01E-04	U-238	2.95E-01	Am-243	3.27E-07
Eu-154	5.07E-06	Np-236	1.49E-11	Cm-242	3.88E-11
Eu-155	1.19E-06	Np-237	1.43E-04	Cm-243	9.57E-10
Tb-159	7.76E-07	Pu-236	2.26E-10	Cm-244	1.48E-05
Tb-160	2.34E-31	Pu-237	6.66E-45	Cm-245	4.37E-10
Tl-206	8.54E-30	Pu-238	8.92E-04	Cm-246	1.95E-11
Tl-207	1.17E-20	Pu-239	2.32E-03	Cm-247	7.96E-14
Tl-208	9.08E-17	Pu-240	4.27E-04	Cm-248	1.82E-15
Tl-209	5.46E-25				
	Total	1.46E+00 G/Gal			

Table 7

Chemical Composition of Feed from Salt Cell

Component	Water Free wt%
$(BC_6H_5O)_3$	0.91
$(C_6H_5)_2$	5.03
$Al(OH)_3$	0.76
$C_6H_5B(OH)_2$	6.07
$C_6H_5HgCOOH$	1.31
C_6H_5OH	2.07
$CsCOOH$	0.50
$Cu(COOH)_2$	1.33
$Fe(OH)_3$	0.80
H_3BO_3	19.02
$HCOOH$	1.36
$KCOOH$	28.86
NH_4COOH	1.08
$Na_2C_2O_4$	1.58
Na_2SO_4	2.39
$NaAl(OH)_4$	2.14
$NaCOOH$	13.10
$NaNO_3$	5.02
$NaTi_2O_5H$	5.72
Others	0.95
Total	100.00

Table 8

Radionuclide Content of Feed from Salt Cell

Isotope	Ci/Gal	Isotope	Ci/Gal	Isotope	Ci/Gal
H-3	9.57E-05	Sb-124	9.51E-30	Tb-160	2.83E-27
C-14	7.45E-11	Sb-125	1.61E-02	Tl-208	2.86E-08
Co-60	3.51E-04	Sb-126	3.45E-05	U-232	1.79E-07
Ni-59	2.41E-07	Sb-126m	2.46E-04	U-233	2.62E-11
Ni-63	2.92E-05	Te-125m	2.31E-07	U-234	8.94E-07
Se-79	4.01E-07	Te-127	1.04E-19	U-235	1.59E-09
Rb-87	2.41E-10	Te-127m	1.06E-19	U-236	1.14E-08
Sr-89	8.48E-32	I-129	1.62E-10	U-238	1.06E-07
Sr-90	4.27E-01	Cs-134	1.78E-01	Np-236	2.10E-13
Y-90	4.42E-01	Cs-135	8.96E-05	Np-237	1.08E-07
Y-91	5.27E-28	Cs-137	3.85E+01	Pu-236	1.28E-07
Zr-93	4.37E-07	Ba-137m	3.69E+01	Pu-237	8.61E-41
Zr-95	6.70E-26	Cs-141	2.32E-50	Pu-238	1.63E-02
Nb-94	9.75E-10	Ce-142	3.89E-11	Pu-239	1.54E-04
Nb-95	1.41E-25	Ce-144	5.47E-06	Pu-240	1.04E-04
Nb-95m	8.28E-28	Pr-144	5.49E-06	Pu-241	1.24E-02
Tc-99	7.46E-05	Pr-144m	6.57E-08	Pu-242	1.47E-07
Ru-103	4.13E-41	Nd-144	1.98E-15	Am-241	2.57E-04
Ru-106	3.36E-05	Pm-147	7.03E-03	Am-242	1.66E-07
Rh-103m	4.01E-41	Pm-148	6.76E-43	Am-242m	1.67E-07
Rh-106	3.37E-05	Pm-148m	9.80E-42	Am-243	6.98E-08
Pd-107	1.47E-07	Sm-147	3.59E-11	Cm-242	1.37E-07
Ag-110m	3.40E-10	Sm148	8.10E-17	Cm-243	5.29E-08
Cd-113	5.60E-20	Sm-149	2.48E-17	Cm-244	1.29E-03
Cd-115m	3.01E-40	Sm-151	3.23E-03	Cm-245	8.06E-11
Sn-121m	4.21E-05	Eu-152	1.14E-05	Cm-246	6.42E-12
Sn-123	1.30E-12	Eu-154	1.47E-03	Cm-247	7.90E-18
Sn-126	2.46E-04	Eu-155	5.93E-04	Cm-248	8.28E-18

Total activity	7.65E+01 Ci/Gal
Decay heat	
Total primary	4.63E-02 Watt/Gal
Total gammas	1.32E-01 Watt/Gal

Table 9

Partial Isotopic Content of Feed from Salt Cell

Isotope	G/Gal	Isotope	G/Gal	Isotope	G/Gal
H-3	9.97E-09	Ru-106	1.00E-08	Te-126	1.43E-09
C-14	1.67E-11	Rh-103	1.06E-03	Te-127	3.94E-26
Co-60	3.10E-07	Rh-103m	1.23E-48	Te-127m	1.13E-23
Ni-59	2.99E-06	Rh-106	9.47E-15	Te-128	3.89E-07
Ni-63	4.94E-07	Pd-104	1.15E-04	Te-129	1.86E-60
Se-77	9.24E-07	Pd-105	9.14E-04	Te-129m	2.01E-57
Se-78	2.33E-06	Pd-106	6.02E-04	Te-130	1.41E-06
Se-79	5.75E-06	Pd-107	2.87E-04	I-127	2.47E-07
Se-80	1.37E-05	Pd-108	1.69E-04	I-129	9.16E-07
Se-82	2.77E-05	Pd-110	5.89E-05	Cs-133	6.16E-01
Rb-85	1.12E-03	Ag-109	1.11E-02	Cs-134	1.37E-04
Rb-87	2.75E-03	Ag-110m	7.16E-14	Cs-135	7.77E-02
Sr-88	2.73E-03	Cd-110	7.42E-07	Cs-137	4.45E-01
Sr-89	2.91E-36	Cd-111	3.49E-06	Ba-134	4.09E-04
Sr-90	3.13E-03	Cd-112	2.41E-06	Ba-136	3.62E-05
Y-89	1.59E-03	Cd-113	1.64E-07	Ba-137	3.46E-03
Y-90	8.11E-07	Cd-114	3.93E-06	Ba-137m	6.85E-08
Y-91	2.15E-32	Cd-115m	1.18E-44	Ba-138	1.23E-02
Zr-90	3.05E-05	Cd-116	1.81E-06	Ce-140	1.72E-03
Zr-91	9.76E-05	Sn-116	4.00E-04	Ce-141	8.15E-55
Zr-92	1.00E-04	Sn-117	2.07E-03	Ce-142	1.62E-03
Zr-93	1.74E-04	Sn-118	2.22E-03	Ce-144	1.71E-09
Zr-94	1.11E-04	Sn-119	2.16E-03	Pr-141	1.61E-03
Zr-95	3.12E-30	Sn-120	2.25E-03	Pr-144	7.26E-14
Zr-96	1.16E-04	Sn-121m	7.83E-07	Pr-144m	3.62E-16
Nb-94	5.20E-09	Sn-122	2.51E-03	Nd-142	5.75E-06
Nb-95	3.60E-30	Sn-123	1.58E-16	Nd-143	1.93E-03
Nb-95m	2.18E-33	Sn-124	3.75E-03	Nd-144	1.67E-03
Mo-95	2.46E-03	Sn-126	8.67E-03	Nd-145	1.07E-03
Mo-96	9.98E-06	Sb-121	3.50E-04	Nd-146	8.67E-04
Mo-97	2.35E-03	Sb-123	4.42E-04	Nd-148	5.00E-04
Mo-98	2.42E-03	Sb-124	5.43E-34	Nd-150	2.01E-04
Mo-100	2.59E-03	Sb-125	1.56E-05	Pm-147	7.57E-06
Tc-99	4.40E-03	Sb-126	4.12E-10	Pm-148	4.11E-48
Ru-100	2.68E-05	Sb-126m	3.13E-12	Pm-148m	4.59E-46
Ru-101	2.06E-03	Te-122	3.08E-10	Sm-147	1.54E-03
Ru-102	2.28E-03	Te-124	1.43E-10	Sm-148	2.65E-04
Ru-103	1.28E-45	Te-125	4.32E-08	Sm-149	1.03E-04
Ru-104	1.15E-03	Te-125m	1.28E-11	Sm-150	1.47E-03
Sm-151	1.23E-04	U-232	8.33E-09	Pu-241	1.23E-04
Sm-152	5.28E-04	U-233	2.72E-09	Pu-242	3.74E-05
Sm-154	9.40E-05	U-234	1.43E-04	Am-241	7.48E-05
Eu-151	5.59E-06	U-235	7.35E-04	Am-242	2.05E-13

Table 9 Contd

Partial Isotopic Content of Feed from Salt Cell

Isotope	G/Gal	Isotope	G/Gal	Isotope	G/Gal
Eu-152	6.48E-08	U-236	1.76E-04	Am-242m	1.71E-08
Eu-153	1.09E-04	U-238	3.16E-01	Am-243	3.50E-07
Eu-154	5.43E-06	Np-236	1.59E-11	Cm-242	4.15E-11
Eu-155	1.27E-06	Np-237	1.53E-04	Cm-243	1.02E-09
Tb-159	8.31E-07	Pu-236	2.42E-10	Cm-244	1.59E-05
Tb-160	2.50E-31	Pu-237	7.13E-45	Cm-245	4.68E-10
Tl-206	9.15E-30	Pu-238	9.55E-04	Cm-246	2.09E-11
Tl-207	1.25E-20	Pu-239	2.49E-03	Cm-247	8.52E-14
Tl-208	9.72E-17	Pu-240	4.57E-04	Cm-248	1.95E-15
Tl-209	5.85E-25				
	Total	1.56E+00 G/Gal			

Table 10

Chemical Composition of Sludge-Precipitate Glass

Component	Water Free wt%
Ag	0.05
Al_2O_3	3.96
B_2O_3	10.28
$BaSO_4$	0.14
$Ca_3(PO_4)_2$	0.07
CaO	0.85
$CaSO_4$	0.08
Cr_2O_3	0.12
Cs_2O	0.08
CuO	0.19
Fe_2O_3	7.04
FeO	3.12
K_2O	3.58
Li_2O	3.16
MgO	1.36
MnO	2.00
Na_2O	11.00
Na_2SO_4	0.36
NaCl	0.19
NaF	0.07
NiO	0.93
PbS	0.07
SiO_2	45.57
ThO_2	0.21
TiO_2	0.99
U_3O_8	2.20
Zeolite	1.67
ZnO	0.08
Others	0.58
Total	100.00

Table 11

Radionuclide Content of Sludge-Precipitate Glass

Isotope	Ci/Lb	Isotope	Ci/Lb	Isotope	Ci/Lb
Cr-51	2.51E-20	Te-125m	7.44E-02	Eu-155	1.28E-01
Co-60	4.58E-02	Te-127	3.24E-05	Eu-156	1.41E-35
Ni-59	6.46E-06	Te-127m	3.31E-05	Tb-160	3.02E-10
Ni-63	8.02E-04	Te-129	8.23E-16	Tl-208	3.04E-07
Se-79	4.58E-05	Te-129m	1.28E-15	U-232	3.61E-06
Rb-87	2.35E-10	Cs-134	9.09E-02	U-233	4.27E-10
Sr-89	1.15E-08	Cs-135	2.68E-05	U-234	9.24E-06
Sr-90	1.26E+01	Cs-136	2.11E-43	U-235	4.24E-08
Y-90	1.29E+01	Cs-137	1.17E+01	U-236	3.04E-07
Y-91	2.04E-07	Ba-136m	2.32E-42	U-238	2.83E-06
Zr-93	3.01E-04	Ba-137m	1.12E+01	Np-236	4.70E-12
Zr-95	2.71E-06	Ba-140	2.76E-40	Np-237	2.40E-06
Nb-94	2.60E-08	La-140	1.16E-40	Pu-236	3.29E-05
Nb-95	5.70E-06	Ce-141	9.68E-15	Pu-237	2.41E-15
Nb-95m	3.36E-08	Ce-142	2.59E-09	Pu-238	4.00E-01
Tc-99	8.30E-04	Ce-144	2.66E+00	Pu-239	3.48E-03
Ru-103	4.54E-12	Pr-143	3.23E-38	Pu-240	2.34E-03
Ru-106	6.07E-01	Pr-144	2.66E+00	Pu-241	4.50E-01
Rh-103m	4.41E-12	Pr-144m	3.20E-02	Pu-242	3.30E-06
Rh-106	6.09E-01	Nd-144	1.31E-13	Am-241	2.97E-03
Pd-107	3.97E-06	Nd-147	3.40E-48	Am-242	3.87E-06
Ag-110m	3.39E-05	Pm-147	6.52E+00	Am-242m	3.90E-06
Cd-113	1.35E-17	Pm-148	1.88E-14	Am-243	1.56E-06
Cd-115m	3.27E-13	Pm-148m	2.72E-13	Cm-242	9.42E-06
Sn-121m	2.13E-05	Sm-147	5.39E-10	Cm-243	1.50E-06
Sn-123	6.87E-05	Sm-148	1.56E-15	Cm-244	2.90E-02
Sn-126	1.19E-04	Sm-149	4.80E-16	Cm-245	1.81E-09
Sb-124	1.92E-11	Sm-151	6.68E-02	Cm-246	1.44E-10
Sb-125	2.29E-01	Eu-152	9.94E-04	Cm-247	1.78E-16
Sb-126	1.66E-05	Eu-154	1.67E-01	Cm-248	1.85E-16
Sb-126m	1.19E-04				

Total activity	6.31E+01 Ci/Lb
Decay heat	
Total primary	1.42E-01 Watts/Lb
Total gammas	4.45E-02 Watts/Lb

Table 12

Partial Isotopic Content of Sludge-Precipitate Glass

Isotope	G/Lb	Isotope	G/Lb	Isotope	G/Lb
Cr-51	2.72E-25	Rh-103	2.34E-02	Te-126	3.62E-05
Co-60	4.05E-05	Rh-103m	1.35E-19	Te-127	1.23E-11
Ni-59	7.99E-05	Rh-106	1.71E-10	Te-127m	3.50E-09
Ni-63	1.36E-05	Pb-104	3.09E-03	Te-128	9.86E-03
Se-77	1.06E-04	Pd-105	2.46E-02	Te-129	3.93E-23
Se-78	2.67E-04	Pd-106	1.58E-02	Te-129m	4.25E-20
Se-79	6.57E-04	Pd-107	7.71E-03	Te-130	3.57E-02
Se-80	1.57E-03	Pd-108	4.55E-03	Cs-133	1.84E-01
Se-82	3.17E-03	Pd-110	1.58E-03	Cs-134	7.02E-05
Rb-85	1.09E-03	Ag-109	5.13E-03	Cs-135	2.33E-02
Rb-87	2.68E-03	Ag-110m	7.14E-09	Cs-136	2.85E-48
Sr-88	6.25E-02	Cd-110	1.79E-04	Cs-137	1.35E-01
Sr-89	3.96E-13	Cd-111	8.42E-04	Ba-134	8.93E-03
Sr-90	9.20E-02	Cd-112	5.81E-04	Ba-136	9.47E-04
Y-89	4.25E-02	Cd-113	3.97E-05	Ba-136m	8.56E-54
Y-90	2.37E-05	Cd-114	9.46E-04	Ba-137	3.63E-02
Y-91	8.31E-12	Cd-115m	1.28E-17	Ba-137m	2.08E-08
Zr-90	8.47E-03	Cd-116	4.37E-04	Ba-138	3.23E-01
Zr-91	6.72E-02	Sn-116	1.93E-04	Ba-140	3.79E-45
Zr-92	6.90E-02	Sn-117	9.98E-04	La-139	1.16E-01
Zr-93	1.20E-01	Sn-118	1.07E-03	La-140	2.09E-46
Zr-94	7.66E-02	Sn-119	1.04E-03	Ce-140	1.15E-01
Zr-95	1.26E-10	Sn-120	1.08E-03	Ce-141	3.40E-19
Zr-96	7.69E-02	Sn-121m	3.97E-07	Ce-142	1.08E-01
Nb-94	1.39E-07	Sn-122	1.21E-03	Ce-144	8.33E-04
Nb-95	1.46E-10	Sn-123	8.36E-09	Pr-141	1.07E-01
Nb-95m	8.84E-14	Sn-124	1.82E-03	Pr-143	4.80E-43
Mo-95	7.37E-02	Sn-125	4.82E-62	Pr-144	3.52E-03
Mo-96	2.99E-04	Sn-126	4.17E-03	Pr-144m	1.76E-10
Mo-97	7.05E-02	Sb-121	4.96E-04	Nd-142	3.81E-04
Mo-98	7.24E-02	Sb-123	6.28E-04	Nd-143	1.28E-01
Mo-100	7.73E-02	Sb-124	1.10E-15	Nd-144	1.10E-01
Tc-99	4.89E-02	Sb-125	2.22E-04	Nd-145	7.08E-02
Ru-100	5.16E-04	Sb-126	1.98E-10	Nd-146	5.75E-02
Ru-101	5.95E-02	Sb-126m	1.51E-12	Nd-147	4.23E-53
Ru-102	4.40E-02	Te-122	7.82E-06	Nd-148	3.33E-02
Ru-103	1.40E-16	Te-124	3.64E-06	Nd-150	1.33E-02
Ru-104	2.22E-02	Te-125	8.30E-04	Pm-147	7.03E-03
Ru-106	1.81E-04	Te-125m	4.13E-06	Pm-148	1.14E-19
Pm-148m	1.27E-17	Tl-206	9.01E-30	Pu-239	5.61E-02
Sm-147	2.32E-02	Tl-207	1.04E-19	Pu-240	1.03E-02
Sm-148	5.10E-03	Tl-208	1.03E-15	Pu-241	4.46E-03
Sm-149	2.00E-03	Tl-209	3.12E-24	Pu-242	8.42E-04

Table 12 Contd

Partial Isotopic Content of Sludge-Precipitate Glass

Isotope	G/Lb	Isotope	G/Lb	Isotope	G/Lb
Sm-150	2.83E-02	U-232	1.68E-07	Am-241	8.64E-04
Sm-151	2.54E-03	U-233	4.43E-08	Am-242	4.79E-12
Sm-152	1.02E-02	U-234	1.48E-03	Am-242m	4.01E-07
Sm-154	1.80E-03	U-235	1.96E-02	Am-243	7.85E-06
Eu-151	1.06E-04	U-236	4.70E-03	Cm-242	2.84E-09
Eu-152	5.63E-06	U-238	8.43E+00	Cm-243	2.91E-08
Eu-153	5.56E-03	Np-236	3.56E-10	Cm-244	3.59E-04
Eu-154	6.20E-04	Np-237	3.40E-03	Cm-245	1.05E-08
Eu-155	2.76E-04	Pu-236	6.19E-08	Cm-246	4.69E-10
Eu-156	2.57E-40	Pu-237	2.00E-19	Cm-247	1.91E-12
Tb-159	5.53E-05	Pu-238	2.34E-02	Cm-248	4.36E-14
Tb-160	2.68E-14				
	Total	1.15E+01 G/Lb			

Table 13A

Chemical Composition of Glass Frits, wt%

	Frit Number					
Oxide	18	21	131	165	200[a]	202
SiO_2	52.5	52.5	57.9	68.0	70.5	77.0
Na_2O	22.5	18.5	17.7	13.0	10.4	6.0
TiO_2	10.0	10.0	1.0	-	-	-
B_2O_3	10.0	10.0	14.7	10.0	12.1	8.0
Li_2O	-	4.0	5.7	7.0	5.0	7.0
MgO	-	-	2.0	1.0	2.0	2.0
ZrO2	-	-	0.5	1.0	-	-
La_2O_3	-	-	0.5	-	-	-
CaO	5.0	5.0	-	-	-	-

[a] Design basis frit.

Table 13B

Projected DWPF Waste Glass Compositions, wt %

Major Glass Components	Constituent Sludge Type						
	Blend	Batch 1	Batch 2	Batch 3	Batch 4	HM	Purex
Al_2O_3	3.98	4.87	4.46	3.25	3.32	7.08	2.89
B_2O_3	8.01	7.69	7.70	7.69	8.11	6.94	10.21
$BaSO_4$	0.27	0.22	0.24	0.26	0.38	0.18	0.29
CaO	0.97	1.17	1.00	0.93	0.83	1.00	1.02
$CaSO_4$	0.077	0.12	0.11	0.10	0.0034	trace	0.12
Cr_2O_3	0.12	0.10	0.12	0.13	0.14	0.086	0.14
CuO	0.44	0.40	0.41	0.40	0.46	0.25	0.42
Fe_2O_3	6.95	8.39	7.11	7.48	7.59	4.95	8.54
FeO	3.11	3.72	3.15	3.31	3.36	2.19	3.78
GroupA[a]	0.14	0.099	0.14	0.10	0.20	0.20	0.078
Group B[b]	0.36	0.22	0.44	0.25	0.60	0.89	0.084
K_2O	3.86	3.49	3.50	3.47	3.99	2.14	3.58
Li_2O	4.40	4.42	4.42	4.42	4.32	4.62	3.12
MgO	1.35	1.36	1.35	1.35	1.38	1.45	1.33
MnO	2.03	2.06	1.62	1.81	3.08	2.07	1.99
Na_2O	8.73	8.62	8.61	8.51	8.88	8.17	12.14
Na_2SO_4	0.10	0.10	0.12	0.096	0.13	0.14	0.12
NaCl	0.19	0.31	0.23	0.22	0.090	0.093	0.26
NiO	0.89	0.75	0.90	1.07	1.09	0.40	1.21
SiO_2	50.20	49.81	50.17	49.98	49.29	54.39	44.56
ThO_2	0.19	0.36	0.63	0.77	0.24	0.55	0.011
TiO_2	0.90	0.66	0.67	0.66	1.02	0.55	0.65
U_3O_8	2.14	0.53	2.30	3.16	0.79	1.01	2.89

[a] Tc, Se, Te, Rb, and Mo.

[b] Ag, Cd, Cr, Pd, Tl, La, Ce, Pr, Pm, Nd, Sm, Tb, Sn, Sb, Co, Zr, Nb, Eu, Np, Am, and Cm.

Table 14

Physical Properties of Glass Wasteforms

Property	Value
Thermal conductivity at 100°C	0.55 Btu/(hr)(ft) (°F)
Heat capacity at 100°C	0.22 cal/(g)(°C) also Btu/(lb)(°F)
Fractional thermal expansion[a]	1.2 x 10-5/°C
Young's modulus	9×10^6 psi
Tensile strength	9×10^3 psi
Compressive strength	1×10^5 psi
Poisson's ratio	0.2
Density at 100°C[a]	2.75 ± 0.05 g/cc
Softening point	488°C

[a] Experimentally determined for Frit 131 and Frit 165 glasses containing composite waste.

Table 15

Composition of Simulated Wastes

Component	Simulation 1[a]	Simulation 2[a]	Simulation 3[a]
Fe_2O_3	47.3	13.8	59.1
MnO_2	13.6	11.3	4.0
Zeolite[b]	10.2	10.2	9.7
Al_2O_3	9.5	49.3	1.4
NiO	5.8	2.0	10.1
SiO_2	4.1	4.5	2.9
CaO	3.5	0.9	4.0
Na_2O	3.1	5.0	5.9
Coal	2.3	2.3	2.1
Na_2SO_4	0.6	0.7	0.8
Glassformer/ waste ratio	70.2/29.8	71.3/27.7	70.2/29.8

[a] Simulation 1 is composite waste; simulation 2 is high aluminum waste; simulation 3 is high iron waste.

[b] Zeolite composition is given in Table 18.

Table 16

Heat Capacities of Simulated Waste Glasses

	Heat Capacity - c_{pt} (cal/(g)(°C))			
Temperature, °C	Calculated Simulation 1 (Composite)	Measured Simulation 1 (Composite)	Measured Simulation 2 (High Al)	Measured Simulation 3 (High Fe)
0		0.186		
50	-	0.20	0.19	0.20
100	0.237	0.21	0.21	0.21
200	0.271	0.23	0.23	0.23
300	0.296	0.27	0.25	0.25
400	0.314			
500	0.328			
600	0.338			
700	0.346			
800	0.353			
900	0.359			
950	0.361			
1000	0.363			
1025	0.364			
1050	0.365			
1075	0.366			
1100	0.367			
1125	0.368			
1150	0.369			
1175	0.369			
1200	0.370			
1250	0.372			
1300	0.373			

Table 17

Measured Density of SRP Simulated Waste Glasses

Glass	Density, g/cm3 at 25°C
Simulation 1 - composite	2.75
Simulation 2 - high Al	2.56
Simulation 3 - high Fe	2.92

Table 18

Zeolite Composition

Component	Wt %
SiO_2	48.0
H_2O	19.1
Al_2O_3	18.6
CaO	10.2
Na_2O	4.1

Table 19

Canister Decay Heat and Activity

Year	Design Basis Curies/Can	Waste Glass Watts/Can
5	233,000	690
10	171,000	517
20	129,000	406
30	101,000	324
40	80,000	262
50	63,000	211
60	50,000	171
70	39,000	139
80	31,000	115
90	25,000	94
100	20,000	78
200	2,200	17
300	400	7.2
400	160	4.1
500	96	2.7
600	70	2.0
700	57	1.6
800	49	1.4
900	45	1.2
1000	41	1.1

Table 20

Radiation from Canister of Sludge-Precipitate Glass

Distance, ft	Gamma, R/hr	Neutron, Mead hr	Total, rad hr
Surface	5570	420	5570
1	2190	97	2190
3	900	42	900
5	470	23	470
10	160	7.5	160
20	44	2.5	44
30	20	1.0	20
50	7	0.5	7
75	3	-	3
100	2	-	2

Table 21

Chemical Composition of Sludge-Precipitate Glass for Radiation Calculations[a]

Component	Wt %	Component	Wt %
Al_2O_3	3.96	MnO	2.00
B_2O_3	10.28	SiO_2	46.72
CaO	0.85	TiO_2	0.99
Fe_2O_3	7.04	U_3O_8	2.20
FeO	3.12	Na_2O	12.15
K_2O	3.58	NiO	0.93
Li_2O	3.16	Zeolite[b]	1.67
MgO	1.36		

[a] Compounds present at >0.8 wt %.
[b] Zeolite composition is given in Table 18.

Table 22

Source Terms for Sludge-Precipitate Glass for Radiation Calculations

Isotope	Ci/Lb	Neutron Yields, n/s/canister	
		a,n	SF
U-232	3.61E-06	6.811E-02	1.207E-03
U-233	4.27E-10	8.056E-02	2.104E-07
U-234	9.24E-06	1.743E+03	4.196E-02
U-235	4.24E-08	7.999	3.167E-02
U-236	3.04E-07	5.735E+01	1.321E-01
U-238	2.83E-06	5.339E+02	5.764E+02
Np-237	2.40E-06	4.528E+02	1.908E-03
Pu-236	3.29E-05	6.207E+03	9.927
Pu-233	4.00E-01	7.547E+07	2.732E+05
Pu-239	3.48E-03	6.565E+05	5.672
Pu-240	2.34E-03	4.415E+05	4.346E+04
Pu-241	4.50E-01	2.080E+03	0.0
Pu-242	3.30E-06	6.226E+02	6.834E+03
Am-241	2.97E-03	5.603E+05	4.156
Am-242	3.87E-06	0.0	0.0
Am-242m	3.90E-06	3.502	2.307E-01
Am-243	1.56E-06	2.943E+02	2.136E-02
Cm-242	9.42E-06	1.777E+03	2.563E+02
Cm-243	1.50E-06	2.830E+02	1.588E-08
Cm-244	2.90E-02	5.471E+06	1.450E+07
Cm-245	1.81E-09	3.415E-01	5.740E-09
Cm-246	1.44E-10	2.717E-02	1.400E+01
Cm-247	1.78E-16	3.358E-08	1.032E-12
Cm-248	1.85E-16	3.490E-08	5.075E-03

Table 23

Major Contributing Isotopes to Gamma Dose Rates

Isotope	R/hr at 10 ft	Percent of Dose
Cs/Ba-137	142.1	88.8
Eu-154	4.9	3.1
Co-60	3.1	2.0
Cs-134	3.1	1.9
Ce/Pr-144	2.6	1.6
Ru/Rh-106	2.3	1.4
Sb-125	1.8	1.1
Others	0.1	0.1
Total	160.0	100.0

Table 24

Gamma Radiation from Canister - Comparison of Calculations

Distance From Canister Surface, ft	SRP (ANISN/QAD-CG)[a] R/hr	GA (PATH)[a] R/hr	Westinghouse (SCAP/ANISN-W),[a] R/hr	Bechtel (GRACE-II),[a] R/hr
0	5,570	7,600	11,300	10,970
1	2,190	3,500	4,500	4,760
2	1,500	2,180		2,885
3	900	1,500	1,860	1,920
4	690	1,070		1,350
5	470			990
7	350	490		590
10	160	270		320
15	75	130		155
20	44			89
30	20	34		40
50	7	12		14
75	3	5		6
100	2	3		3

[a] Calculational code used.

Table 25

Neutron Radiation from Canister - Comparison of Calculations

Distance from Canister Surface, ft	SRP (ANISN),[a] mrem/hr	GA (DTF)[a] mrem/hr	Westinghouse (ORIGEN/SOURCES/ANISN/WEST),[a] mrem/hr
0	420	250	305
1	97		
3	42		
5	23		
10	7.5		
20	2.5		
30	1.0		
50	0.5		

[a] Calculational code used.

Table 26

Reference Canister Temperatures[a]

Watts	Surface Temp. °C	Centerline Temp. °C	Surrounding Air Temp. °C
425	34	50	20
510	54	71	38
1000	66	120	38

[a] Reference DWPF sludge-precipitate waste form: canister 24-in. OD by 118 in. high, 22 ft^3 of waste glass containing 28% sludge oxides, and air convection cooling.

Table 27

Projected Waste Inventory and Fission Product Radioactivity as of December 31, 1988

	Volume, (10^3) m^3	Activity (10^6) Ci	Power (10^3) W
Sludge	13.9	495.5	1546.1
Salt Cake	50.4	193.7	501.0
Liquid	62.1	88.8	245.3
Precipitate	0.2	1.3	3.3
Total	126.6	779.3	2295.7

NOTE: 1 m^3 = 264.2 gal.

Isotope	Curies
Sr-89	1,219,000
Sr-90	137,200,000
Y-90[a]	137,300,000
Y-91	2,633,000
Zr-95	4,805,000
Nb-95[a]	10,410,000
Ru-106	5,583,000
Rh-106[a]	5,583,000
Cs-137	141,500,000
Ba-137[a]	130,200,000
Ce-144	70,630,000
Pr-144[a]	70,640,000
Pm-147	60,220,000
Total	777,923,000

[a] Daughter isotopes.

Table 28

Estimated Production Schedule and Estimated Cumulative Average Radioactivity and Thermal Power per Canister of HLW Glass

End of Calendar Year	No. of Canisters Produced During Year	Cumulative No. of Canisters Produced	Cumulative Radioactivity Total, Ci(10^6)	Cumulative Radioactivity Per Canister, Ci	Cumulative Thermal Power Total, W(10^3)	Cumulative Thermal Power Per Canister, W
1991	0	0	--	--	--	--
92	102	102	--	--	--	--
93	410	512	32.9	64,260	87.3	171
94	410	922	52.9	57,380	142.7	155
95	410	1,332	70.0	52,550	190.9	143
96	410	1,742	81.7	46,900	223.5	128
97	410	2,152	91.0	42,290	249.1	116
98	410	2,562	100.5	39,230	275.0	107
99	376	2,938	110.3	37,540	302.1	103
2000	205	3,143	120.1	38,210	329.0	105
01	205	3,348	135.0	40,320	371.8	111
02	205	3,553	158.8	44,690	440.7	124
03	205	3,758	185.0	49,230	516.3	137
04	205	3,963	205.2	51,780	572.9	145
05	205	4,168	218.4	52,400	609.5	146
06	205	4,373	233.8	53,460	653.2	149
07	205	4,578	248.2	54,220	694.6	152
08	205	4,783	264.3	55,260	740.9	155
09	205	4,988	276.1	55,350	774.5	155
2010	205	5,193	283.9	54,670	798.0	154
11	161	5,354	296.4	55,360	835.5	156
12	30	5,384	306.4	56,910	864.9	161
13	31	5,415	313.1	57,820	884.3	163
14	30	5,445	317.5	58,310	896.4	165
15	31	5,476	370.5	58,530	904.4	165
16	30	5,506	323.0	58,660	910.8	165
17	31	5,537	326.0	58,880	918.7	166
18	30	5,567	329.4	59,170	929.2	167
19	31	5,598	336.0	60,020	949.6	170
2020	30	5,628	343.5	61,030	971.5	173
21	31	5,659	348.6	61,600	986.0	174
22	30	5,689	347.5	61,080	982.7	173

Calculated from estimates provided for 1988 Integrated Data Base. Year-by-year radioactivity and thermal power per canister do not necessarily represent actual processing schedules and tankage allocations. Radioactivity and thermal power shown are for fission products only. Radioactivity will be about 1% higher and thermal power about 6% higher when actinides are included.